

¹ Mechanisms behind facilitation-competition transition along ² rainfall gradients

³ Oded Hollander^{*1}, Yair Mau^{†2}, and Niv DeMalach^{‡1}

⁴ ⁵¹Institute of Plant Sciences and Genetics in Agriculture, Faculty of Agriculture Food and Environment, The Hebrew University of Jerusalem, Rehovot, Israel

⁶ ⁷ ²Department of Soil and Water Sciences, Robert H. Smith Faculty of Agriculture,
Food and Environment, The Hebrew University of Jerusalem, Rehovot, Israel

Keywords: Stress gradient hypothesis, Aridity gradient, Precipitation, Plant-Plant interactions, consumer-resource model, shading, woody-herbaceous interactions, dryland ecosystems, ecosystem engineers

*Contributing author. E-mail: oded.hollander@mail.huji.ac.il

[†]*Corresponding author. E-mail: yair.mau@mail.huji.ac.il

[†]*Corresponding author. E-mail: niv.demalach@mail.huji.ac.il

[†]These authors contributed equally to this work.

11

Abstract

12

Woody cover is rapidly changing due to mortality, shrub encroachment, and afforestation, 13
reshaping herbaceous communities and ecosystem functioning worldwide. Often, trees and shrubs 14
promote herb growth in dry sites but suppress it in wetter ones, as predicted by the classical 15
Stress Gradient Hypothesis. However, explanations for the facilitation-to-competition transition 16
remain verbal and contested, lacking a clear link to resource competition theory. Here, we 17
present a mechanistic framework consisting of two submodels: (i) canopy shading that reduces 18
photosynthesis and evapotranspiration, and (ii) root effects, including water uptake and increased 19
moisture via hydraulic redistribution. We elucidate the conditions under which interactions shift 20
from facilitation to competition. The models reproduce this reversal only when water is not the 21
sole limiting factor at high rainfall or when woody density increases with precipitation. Moreover, 22
the reversal can occur across any aridity gradient, including those driven by evaporative demand 23
influenced by temperature and humidity. The two pathways leave distinct signatures: canopy 24
shading produces a hump-shaped pattern with maximum facilitation at intermediate stress, while 25
the root pathway predicts a shift from positive to negative interactions as water availability 26
increases. By translating a classic idea into a quantitative framework, this model enhances 27
ecosystem management in a changing world.

28 1 Introduction

29 Global climate and land-use changes are rapidly reshaping woody vegetation worldwide^{1;2}. These shifts
30 are especially common in drylands, which cover about 40% of Earth's land surface^{3;4}. Many water-
31 limited systems are losing woody cover due to widespread drought and fire⁵. Conversely, other dry
32 regions show woody expansion, driven by shrub encroachment^{2;6} and large-scale afforestation aimed at
33 climate mitigation^{1;7}. In these ecosystems, woody plants (hereafter, trees) strongly shape microclimate
34 and resource availability, thereby influencing the abundance and distribution of herbaceous plants
35 (hereafter, herbs) that sustain forage production and biodiversity in drylands^{2;6}.

36 Trees are ecosystem engineers, altering the environment beyond simply consuming light and water⁸.
37 They can facilitate herb growth through **canopy and root mechanisms**. The canopy suppresses light
38 availability, which reduces carbon assimilation (photosynthesis) but also lowers evapotranspiration and
39 therefore water loss⁹. This reduction in evapotranspiration also results from microclimatic buffering;
40 slower wind speeds, higher humidity, and lower temperatures beneath the canopy¹⁰. Tree roots not only
41 extract water, thereby drying the soil, but can also increase soil moisture by enhancing infiltration¹¹
42 and redistributing water from deeper to shallower soil layers through hydraulic lift^{12;13}.

43 Rainfall amount often mediates the balance between these positive and negative effects. Meta-analyses
44 find that trees typically benefit herbs at low rainfall but hinder them as rainfall increases^{14–16}. Even
45 so, some studies report inconsistent neighbor effects along similar gradients¹⁷, pointing to hidden
46 thresholds or additional factors that alter the expected pattern.

47 Over the past three decades, the transition from facilitation to competition has largely been investigated
48 through the lens of the Stress Gradient Hypothesis (SGH). This conceptual framework was proposed to
49 explain why facilitation dominates under high abiotic stress (low rainfall), whereas competition prevails
50 under benign conditions^{18–23}. The original explanations emphasized plant responses along water-stress
51 gradients²⁰, but the hypothesis has since been applied to many other stress types^{24;25}. The primary
52 argument is that tree-mediated relief of water stress dominates under low rainfall, whereas shading-
53 induced inhibition dominates under low stress (high rainfall)⁹. These verbal arguments were later
54 extended using phenomenological models that embedded spatial-temporal dynamics²⁶ and biodiversity
55 feedbacks²⁷.

56 Despite its prominence, the SGH has been questioned both mechanistically and in terms of predicted
57 patterns^{9;28–31}. Some studies argue that species interactions become more strongly negative with
58 rainfall¹⁴, whereas others report a unimodal (hump-shaped) pattern in which facilitation peaks at
59 intermediate stress and weakens under both severe aridity and benign conditions²⁹. Resolving these
60 discrepancies calls for quantitative models that explicitly represent resource dynamics and make
61 assumptions transparent, allowing specific processes such as shading or water uptake to be identified
62 as drivers that generate, sustain, or limit facilitation along the gradient.

63 Consumer-resource theory is the leading modeling framework for mechanistic explanations of species
64 interactions^{32–35}. Yet, it has only recently been applied to the SGH^{36;37}. These recent applications
65 yielded insights into the role of trees in elevating resource availability during early succession³⁶ and into
66 the joint effects of drought and grazing³⁷. However, they focused exclusively on root mechanisms and
67 did not consider canopy shading, the mechanism emphasized in the classical conceptual hypothesis²⁰.
68 Crucially, and contrary to the SGH's prediction of a facilitation-to-competition shift, these consumer-
69 resource models produced an interaction sign that remained constant (either positive or negative) along
70 the rainfall gradient, rather than a transition from facilitation to competition.

71 Here, we develop a minimal consumer-resource framework that generates the classic shift from
72 facilitation to competition as rainfall (resource supply rate) increases. The model clarifies the

73 conditions under which this transition emerges for both canopy and root mechanisms (Fig. 1)
 74 and reconciles contrasting predictions regarding how facilitation strength varies along precipitation
 75 gradients.

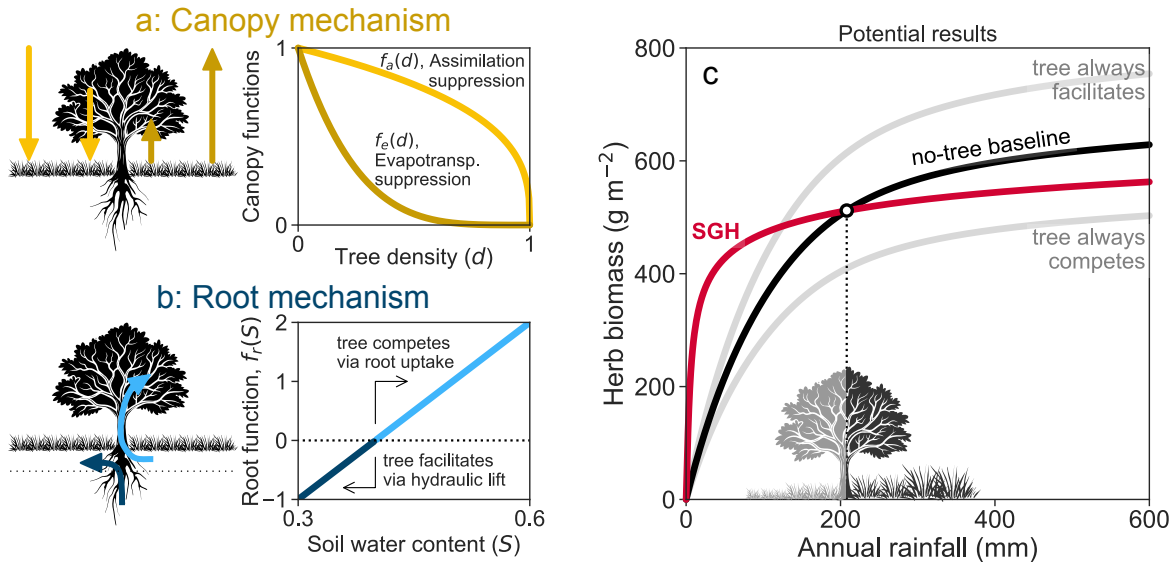


Figure 1: Assumptions of the two submodels (a, b) and potential model outcomes (c).

(a) The canopy mechanism assumes that tree density suppresses both photosynthetic assimilation (yellow) and water loss by evapotranspiration (brown). However, the reduction in evapotranspiration with increasing tree density is greater than the reduction in photosynthesis, which is a necessary condition for facilitation under shading. (b) The root mechanism focuses on water uptake (light blue) and hydraulic lift (dark blue), where water from deep layers is transported upward by the tree and increases moisture in shallow soil. The curve reflects the net effect of these two opposing processes: when the soil is dry, steep water potential gradients between deep and shallow layers favor upward water movement through the roots, producing negative net uptake (a gain to the upper soil). As soil moisture increases, water extraction by roots becomes more efficient, and uptake outweighs hydraulic lift, resulting in higher (more positive) net uptake values. (c) Potential model outcomes are illustrated by comparing rainfall–biomass relationships with and without trees (black line). In the two simple scenarios (grey), trees either consistently facilitate or consistently inhibit herb growth across the rainfall gradient, whereas the Stress Gradient Hypothesis (SGH; red line) predicts a transition from facilitation to competition, marked by the intersection between the black and the red lines.

76 2 Results

77 We developed a consumer-resource model that describes the coupled dynamics of herbs' biomass and
 78 soil moisture as follows:

herb biomass:

$$\frac{dB}{dt} = \overbrace{a f_a(d) f_k(B) B S}^{\text{growth}} - \overbrace{m B}^{\text{mortality}} \quad (1a)$$

soil water:

$$\underbrace{n z_r}_{\text{soil depth}} \frac{dS}{dt} = \underbrace{p}_{\text{precipitation}} - \underbrace{q_s S^\gamma}_{\text{drainage}} - \underbrace{e_0 f_e(d) B S}_{\text{evapotranspiration}} - \underbrace{f_r(S, d)}_{\text{tree root}}. \quad (1b)$$

79 The first equation tracks the change in herb biomass (B) over time, which is governed by growth
 80 and mortality processes. The second equation represents the dynamics of soil moisture (S), which
 81 is influenced by gains from precipitation (p) and losses due to drainage, evapotranspiration, and a
 82 tree-root effect. Due to their much slower dynamics, trees are represented as a constant parameter for
 83 tree density (d representing canopy cover or root density). This parameter affects both the canopy-
 84 suppression factors on herb growth ($f_a(d)$) and on evapotranspiration ($f_e(d)$), as depicted in Fig. 1a.
 85 The impact of the root mechanism $f_r(S, d)$ on soil water is depicted in Fig. 1b. We further assumed
 86 that when water and light are ample, other factors such as nutrients or genetic limits constrain herb
 87 growth, represented by a carrying capacity term $f_k(B) = 1 - B/k$. For simplicity, we investigated each
 88 mechanism separately: when examining canopy effects, we removed root effects, and vice versa.

89 When water is the main limiting factor and tree density is constant, our model, like previous
 90 mechanistic models^{36;37}, shows that the interaction between trees and herbs remains either facilitative
 91 or competitive along the entire precipitation gradient. However, a key finding is that introducing a new
 92 limiting factor ($f_k(B)$ in the model), which can represent nutrient limitation, or a genetic size limit,
 93 is a **necessary condition** for the Stress Gradient Hypothesis transition to occur (see Supplementary
 94 Section S1). When this condition is met, both the canopy and root mechanisms can produce a clear
 95 shift from facilitation to competition as precipitation increases. The following explores how each of
 96 these mechanisms drives this transition.

97 In the **canopy mechanism**, in the absence of trees, herb biomass increases with precipitation, showing
 98 a saturation pattern as the curve's slope decreases (black line in Fig. 2a). With some trees (light
 99 curve), herb biomass is higher than the no-tree baseline at low precipitation but is reduced at higher
 100 precipitation levels, showing a clear transition from facilitation to competition. At very high tree
 101 density (dark curve), herb biomass is suppressed across the entire precipitation gradient.

102 This pattern is a result of a tug of war between two opposing forces exerted by the trees. First,
 103 trees facilitate growth by providing shade, which reduces evapotranspiration and conserves soil water.
 104 This effect is represented by the function $f_e(d)$, leading to greater soil water availability relative to a
 105 no-tree environment (see Fig. 2c). Second, trees inhibit herb's growth by reducing light availability
 106 through the function $f_a(d)$. This factor, along with other limiting elements like nutrients or grazing
 107 (captured by the carrying capacity term, $f_k(B)$), down-regulates herb assimilation. The combined
 108 effect is represented by the product $f_a(d)f_k(B)$.

109 At low precipitation, herb biomass is low, so the carrying capacity term $f_k(B)$ is very weak (close to 1).
 110 In this dry scenario, the tug of war is mainly between the water-saving benefit of $f_e(d)$ and the light
 111 reduction effect of $f_a(d)$. When tree density is low, the extra soil water overpowers the minor loss in
 112 light, facilitating herb growth (light curve in Fig. 2a). However, when tree cover is high, the reduction
 113 in light becomes too strong, suppressing the herbs (dark curve). As precipitation increases, herb
 114 biomass also rises. This strengthens the carrying capacity term $f_k(B)$ (making it closer to zero) and
 115 tips the balance. The combined competitive effect of reduced light and carrying capacity ($f_a(d)f_k(B)$)
 116 becomes stronger than the facilitative effect of water conservation. In other words, under high rainfall,
 117 water is no longer the limiting factor, and therefore, the benefit of reduced water loss is not enough
 118 to compensate for the reduction in photosynthesis, leading to a transition from net facilitation to net
 119 competition.

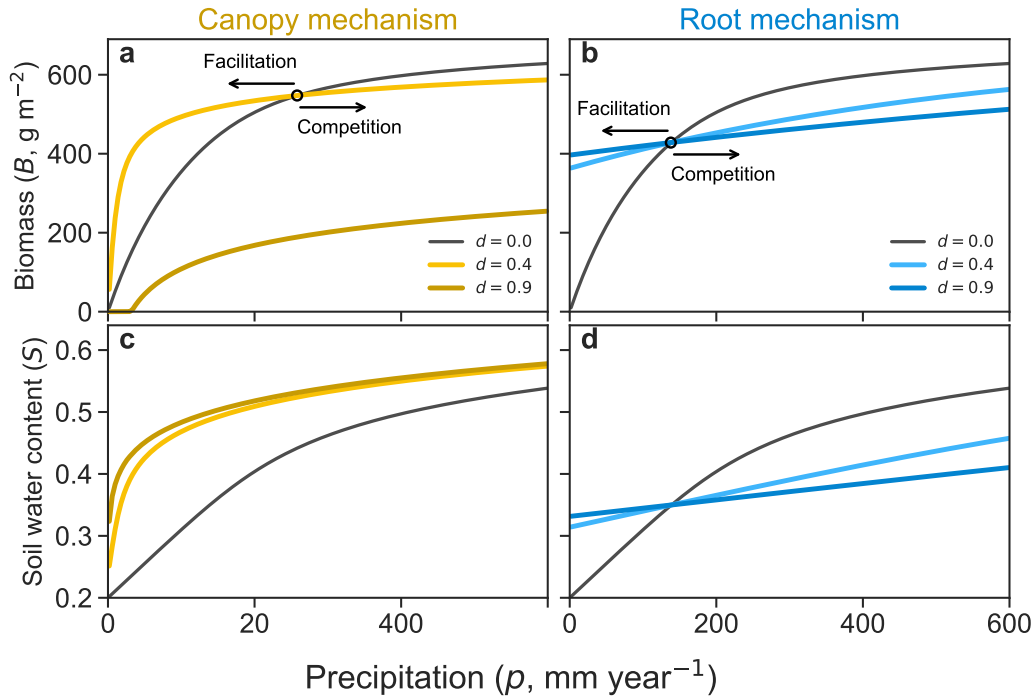


Figure 2: **The transition from facilitation to competition is produced by two different mechanisms.** Herb biomass and soil water solutions of (Eqs. (1)) are shown for the canopy mechanism (panels a,c) and the root mechanism (panels b,d). Black lines give the no-tree baseline ($d = 0$), light solid curves show moderate tree density ($d = 0.4$) and dark solid curves high tree density ($d = 0.9$). Facilitation (competition) occurs when the herb biomass solid curves are above (below) the baseline curve. Other parameter values are as reported in Table 1.

120 For the **root mechanism**, all non-zero tree densities show a similar transition pattern: herb biomass
 121 is higher than the baseline at low precipitation and lower at high precipitation (see Fig. 2b). As tree
 122 density increases, both effects intensify along the precipitation gradient. This is because the tug of
 123 war between facilitation and competition is expressed by a single function, $f_r(S, d)$, which represents
 124 the net effect of tree roots on soil water available in the herb root zone.

125 This function captures the tipping of the balance as soil water content changes. At low soil water
 126 levels, tree roots can lift water from deeper soil layers to the herb root zone, facilitating growth. As
 127 soil water content increases, hydraulic lift is no longer possible. Beyond this point, roots begin to
 128 compete with herbs by taking up water from the same soil layer. Counterintuitively, the root term
 129 $f_r(S, d)$ by itself does not produce a facilitation-to-competition switch (see Supplementary Section S1).
 130 With water as the only limiting resource (i.e., $f_k(B) = 1$), the equilibrium soil moisture S^* is set by the
 131 consumer and is independent of the precipitation supply p (R* logic;³³). Because f_r acts through S
 132 rather than directly through p , the sign of the interaction is fixed by whether S^* lies below or above the
 133 hydraulic switching range, so it does not change along the rainfall gradient. However, when a second
 134 growth constraint is introduced through the carrying-capacity term $f_k(B)$, the outcome changes: as p
 135 increases, biomass approaches its limit and cannot deplete water further, so S^* rises. This upward shift
 136 in S^* carries the system across the hydraulic threshold, turning facilitative lift into competitive uptake
 137 and yielding the observed transition. Put simply, $f_k(B)$ caps biomass at high rainfall, weakening
 138 consumption and allowing soil water to accumulate, which moves S^* into the competitive domain of
 139 $f_r(S, d)$.

140 Notably, the two mechanisms produce very different biomass responses at low precipitation. In the
 141 canopy mechanism, precipitation is the only water source, so all curves must start from the origin,
 142 zero biomass at zero rainfall. A small initial increase in precipitation leads to stronger facilitation,
 143 which is visible as a widening gap between the low-tree-density curve and the no-tree baseline (light
 144 and black curves in Fig. 2a, respectively). This facilitative gap eventually narrows before disappearing
 145 at the transition to competition. In contrast, the root mechanism includes an additional water source:
 146 hydraulic lift from deeper soil layers during dry surface conditions. This allows herb biomass to persist
 147 even without precipitation. The gap between tree-density curves and the baseline shrinks steadily as
 148 precipitation increases, until it reaches the transition point. This distinct pattern in the biomass gap is
 149 key to understanding the contrasting responses in interaction intensity between the two mechanisms.

150 For the canopy mechanism, the interaction intensity based on the absolute difference is unimodal (see
 151 Fig. 3a). This pattern directly results from the widening and eventual vanishing of the gap between
 152 the biomass curve with trees and the no-tree baseline curve, as previously discussed. However, when
 153 using the relative log response ratio (see Fig. 3c), the interaction intensity decreases monotonically
 154 for p below the transition threshold. In contrast, the root mechanism yields monotonically-decreasing
 155 positive interaction intensities, regardless of whether absolute difference or relative log response ratio is
 156 used. A broader discussion of the canopy mechanism's interaction intensity in the full (p, d) parameter
 157 space is given in Supplementary Section S2.

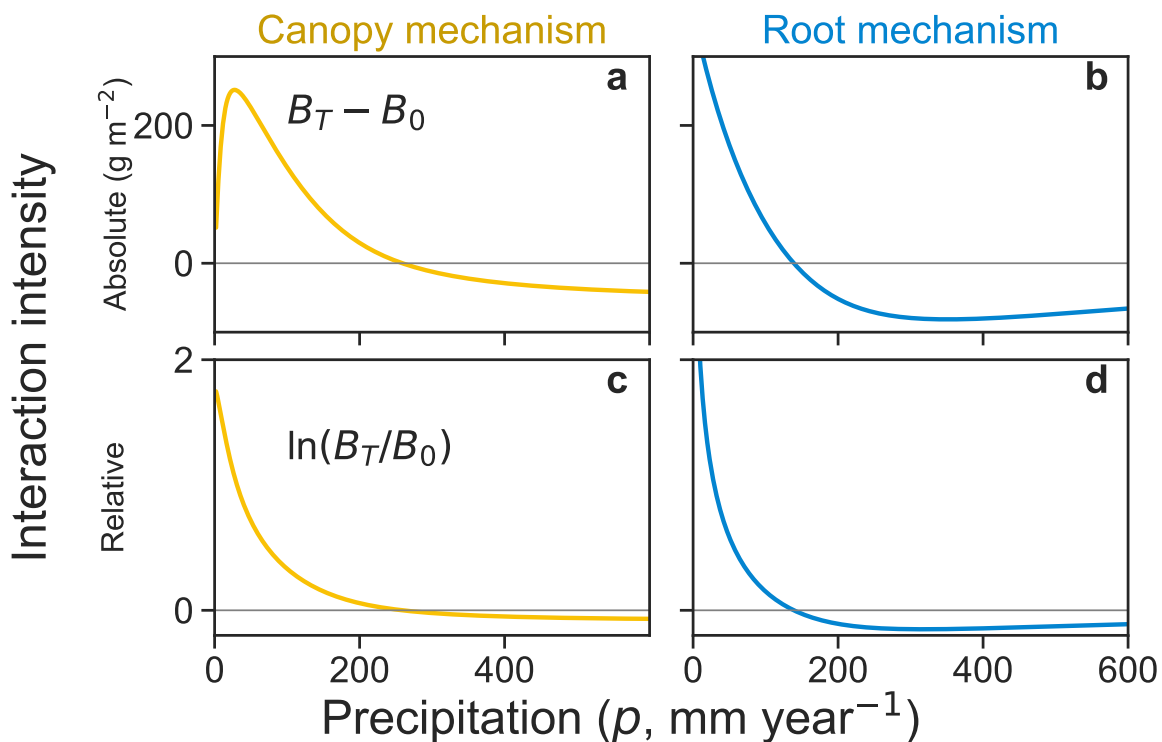


Figure 3: **Interaction intensity patterns depend on both mechanism and metric.** The gray lines represent zero interaction. Positive interactions indicate facilitation by trees; negative interactions indicate competition. Panels a and b show the absolute interaction intensity, $B_T - B_0$, where B_0 and B_T denote herb biomass in the absence and presence of tree density, respectively. Panels c and d show the relative log response ratio, $\ln(B_T/B_0)$. Parameters: $d = 0.0$ and $d = 0.3$ were used to compute B_0 and B_T , respectively; other parameters are given in Table 1.

158 3 Discussion

159 The Stress Gradient Hypothesis has guided decades of work but has largely been articulated in
160 verbal or phenomenological terms^{9;19;20;26;27;29;30}. We show that a minimal consumer-resource model
161 linking canopy shading or root water redistribution to herb biomass generates the observed shift from
162 facilitation to competition along rainfall gradients. Our model also specified when the shift should and
163 should not arise. Finally, the framework also clarifies the expectation on interaction intensity, with a
164 mid-gradient peak in the facilitation under shading and a monotonic decline from positive to negative
165 effect under the root pathway.

166 Our aim is to provide general insight and testable predictions rather than site-specific accurate
167 description. Accordingly, the model is intentionally simple yet mechanistic: water balance is explicit,
168 and interaction signs emerge from the equations rather than being imposed a priori. This simplicity
169 enables a thorough understanding of each parameter (See Supplementary Section S3).

170 The model focuses on the primary pathways through which woody plants influence herbs: canopy
171 shading and root water redistribution. It keeps tree density fixed while examining steady-state
172 contrasts. Other processes, such as grazing protection, nutrient supply, or spatial patterns^{31;36–38}
173 can be incorporated where they are expected to matter (see the Supplementary Sections S4 and S8
174 for transient dynamics and varying tree density). We therefore view this framework as a baseline for
175 systems where water and light competition dominate, and as a foundation for targeted extensions that
176 incorporate additional mechanisms.

177 The stress gradient hypotheses have been invoked for many stress types^{9;18–23}. Yet, as Maestre
178 et al.²⁹ noted, “Stress is not a precise concept, and therefore it is difficult to apply quantitatively
179 to communities or ecosystems”. Here we focus on mechanisms tied directly to plant water balance,
180 while recognizing that other stressors such as freezing, toxicity, or salinity, are likely to require different
181 model structures. The same framework can also be applied to evaporative demand, another driver of
182 aridity, which is influenced by temperature and humidity. This driver can change the magnitude
183 of facilitation and competition and shift the transition point along the gradient. Still, the model
184 consistently predicts a shift from net facilitation to net competition as water limitation relaxes (see
185 Figure in Supplementary Section S5).

186 The model resolves the empirical question whether stress should be represented by resource supply
187 rate (precipitation) or by resource abundance (soil water content)^{9;36;37;39}. It shows that precipitation
188 or evaporative demand are the appropriate measures for quantifying water stress in such systems
189 (see Supplementary Section S6). Soil water content, in contrast, is not an independent driver but an
190 emergent outcome of interacting processes including precipitation, evapotranspiration, biotic uptake,
191 and substrate properties^{9;36;39}. Treating soil water as externally fixed cuts off these mechanistic links
192 and removes the causal connection between resource supply and species interactions. Only when stress
193 is parameterized as a supply rate can the facilitation–competition interplay characteristic of the SGH
194 be captured^{9;36;37;39}.

195 3.1 Canopy mechanism

196 Shading is a ubiquitous factor plant growth and community dynamics^{40–43}. This mechanism is central
197 in conceptual models that generate the transition from facilitation to competition^{9;20}. Our findings
198 indicate that shading can simultaneously enhance and constrain growth, with implications far beyond
199 tree–herb interactions.

200 In the model, shading acts solely by reducing light, so any reduction in radiation, whether caused from
201 trees, slope aspect, buildings, or solar panels, should generate similar responses. In dry conditions,
202 shaded hillslopes, north-facing in the northern hemisphere and the reverse in the southern hemisphere,
203 should be more productive than sun-exposed slopes. In wet conditions, the pattern should reverse.
204 Variation with slope aspect is a long-standing observation in botany^{44;45}, yet we are not aware of
205 a mechanistic model that explains this global pattern. The same logic applies to urban ecosystems,
206 where buildings cast shade, and to agricultural settings, with the co-location of solar panels and crops
207 (agrivoltaics) being on the rise over the last two decades⁴⁶. In such settings, the model predicts when
208 agrivoltaics will increase or decrease productivity depending on environmental conditions

209 The model highlights several conditions that have seldom been investigated in empirical studies along
210 gradients. First, a necessary condition for facilitation under shading is that the proportional reduction
211 in evapotranspiration with increasing shade exceeds the proportional reduction in photosynthesis.
212 Although this likely holds for many plants, there are clear exceptions, such as species that require high
213 light and are sensitive to shade. We therefore suggest that empirical tests of the shading mechanism
214 begin by verifying this assumption.

215 For the transition from facilitation to competition to occur without a change in tree cover, another
216 condition must be met. Under high rainfall, water must cease to be the main limiting factor (the
217 carrying capacity effect). This implies that a qualitative switch is less likely when moving from an arid
218 to a semiarid system if both remain water-limited. Instead, a switch is expected only when crossing
219 into a system limited by another resource, such as nutrients (see Supplementary Section S7, which
220 shows that carrying capacity is equivalent to an additional essential resource). This result may explain
221 empirical studies that do not observe a shift along precipitation gradients^{17;29;47;48} and underscores
222 that the transition should not be viewed as inevitable.

223 Alternatively, shading can lead to a facilitation-to-competition transition without introducing carrying
224 capacity, but only when tree density increases with rainfall (See Supplementary Section S8). This
225 occurs because at high tree cover, light becomes the primary limiting factor and offsets the positive
226 effects of shading on water balance. This density effect can be further enhanced by photoinhibition,
227 where excessive light inhibits photosynthesis. We therefore recommend that future empirical studies
228 quantify how tree density changes along the gradient and manipulate tree cover directly, or mimic
229 shading with shade cloth. Such an approach is necessary to determine whether interaction outcomes
230 change under a constant shade level (Fig. 2), or arise from shifts in canopy density along the gradient
231 (Supplementary Section S8).

232 3.2 Root mechanisms

233 Root-mediated effects in natural settings can be highly variable because they depend on root
234 architecture and soil properties^{11;49}. In the canopy mechanism, we used a two-layer simplification
235 in which deep tree roots do not change the soil water available to herbs⁵⁰. By contrast, in the root
236 mechanism, we assumed partial overlap in rooting depth so that trees and herbs draw from the same
237 near-surface water. We further assumed hydraulic lift, whereby trees move water upward from deeper
238 layers when the surface is dry and draw water from the herb layer when it is wet.

239 When trees increase soil moisture under dry conditions and reduce it under wet conditions, a transition
240 from facilitation to competition can occur. Although we initially expected this transition to arise
241 inevitably from the root mechanism, we found that it occurs only when another factor limits biomass
242 at high rainfall; otherwise, equilibrium soil moisture remains constant along the gradient. Notably,
243 although there is empirical evidence for hydraulic lift¹³, its strength and prevalence remain uncertain,
244 so we treat it as secondary to shading for broad-scale patterns. Alternatively, a more common way

245 trees may increase soil moisture is by enhancing infiltration¹¹. While infiltration alone does not cause
246 a facilitation-to-competition transition³⁷, our model shows that it can do so when combined with
247 shading: under low precipitation, the positive effects of increased infiltration dominate, whereas at
248 high rainfall, the negative effects of shading prevail (Supplementary Section S9).

249 3.3 Concluding Remarks

250 Our findings help reconcile conflicting reports on interaction strength along rainfall gradients by
251 showing that the expected pattern depends first on the mechanism. Under the canopy pathway,
252 the absolute difference in biomass is hump-shaped, with maximum facilitation at intermediate rainfall,
253 whereas under the root mechanism, the interaction declines monotonically from positive to negative.
254 A second source of variation is the metric, and this sensitivity applies to shading in particular: only the
255 absolute measure yields a unimodal pattern, whereas relative measures decline with rainfall, consistent
256 with earlier suggestions⁹.

257 Importantly, tree density further modulates these patterns of interactions along aridity gradients
258 (Supplementary Section S2). Hence, empirical patterns can only be interpreted accurately when tree
259 density is quantified. Under low precipitation, facilitation peaks at intermediate density, while low and
260 high tree densities weaken it. As precipitation increases, progressively lower densities are sufficient to
261 shift the balance from facilitation to competition. Eventually, at high rainfall, even near-zero tree
262 density reduces herb performance, so further changes in density no longer cause a qualitative shift.⁹.

263 Many empirical studies report a shift from facilitation to competition^{14–16}, and many do not^{9;28–31}. In
264 the lens of our framework, cases without a shift arise when (i) other pathways dominate, for example,
265 protection from herbivory, or (ii) when the conditions for a shift are not met, for example, when
266 shade suppresses photosynthesis more than evapotranspiration. This perspective moves the discussion
267 from whether the hypothesis holds to which mechanism operates. It also points to practical tests,
268 pairing shade manipulations with canopy and soil water measurements, and reporting both absolute
269 and proportional changes.

270 Looking ahead, climate change is exacerbating water limitations in many regions^{51–54}, while woody
271 cover is changing due to drought, fire, shrub encroachment, afforestation, and altered land use^{1;2;5–7}.
272 A compact mechanistic framework can help anticipate where shade will enhance herb production by
273 conserving water and where it will suppress production due to light limitations, and it can guide
274 restoration and conservation efforts toward interventions that match local mechanisms. By building
275 on the Stress Gradient Hypothesis and giving it simple, testable conditions, this framework connects
276 a classic idea to actionable predictions for conserving dryland ecosystems in a rapidly changing world.

277 4 Methods

278 We developed a consumer-resource model (see Eq. (1)) that describes the dynamics of herbaceous
279 biomass density (B , kg m⁻²)^{36;37}, and relative soil-water content (S , dimensionless)⁵⁵.

280 The model makes three key assumptions: (i) Tree biomass changes on a much longer time scale than
281 herb biomass, so tree density is treated as constant and remains in quasi steady state relative to the
282 herbs and soil water. (ii) Herb roots occupy only the upper soil layer, whereas tree roots also reach
283 deeper layers, allowing trees to lift water upward or to draw water away from the herb rooting zone;
284 (iii) Herb growth is limited by light and by soil moisture, yet only water can accumulate over time and
285 therefore is described by a balance equation. To incorporate constraints on growth beyond water and

286 light, we include a carrying capacity term, which is equivalent to assuming another limiting resource,
287 such as an essential nutrient (see Supplementary Section S7).

288 The dynamics of herbaceous biomass density B are governed by growth and mortality terms (Eq. (1a)).
289 The dynamics of relative soil-water content S are dictated by a water-balance equation⁵⁵, whose input
290 is precipitation and whose outputs are drainage to deeper soil layers and evapotranspiration, while tree-
291 root processes can function as both inputs and outputs depending on direction of water flow.(Eq. (1b)).
292 Herb biomass and water are averaged over the horizontal dimensions, and water is averaged over the
293 active soil depth nz_r , following a traditional bucket-model approach⁵⁶.

294 The functions $f_a(d)$, $f_k(B)$, $f_e(d)$, $f_r(S, d)$ are modular components of the model that can be turned on
295 or off, either when switching between model variants or when testing the impact of different limiting
296 factors. The features that are common to all realizations of the model are: (i): Herb biomass growth
297 rate is linearly dependent on soil water content S (when the carrying capacity term is negligible). (ii)
298 Herb biomass mortality rate is proportional to biomass. (iii) Evapotranspiration is down-regulated by
299 soil moisture availability, following a linear β function of S ^{57;58}, and is proportional to herb biomass
300 density. (iv) Drainage is modeled by a highly nonlinear function of soil moisture⁵⁹, commonly used in
301 ecohydrological modeling⁶⁰. (v) The logistic growth term $f_k(B) = 1 - B/k$ was used throughout this
302 paper and was only turned off ($f_k(B) = 1$) in Supplementary Sections S1 and S8, where we studied
303 the effects of removing additional limiting growth-limiting factors beyond water and light. (vi) All
304 the model parameters (Table 1) are constant. In particular, precipitation rate p is understood as the
305 total precipitation of the growing season divided by its duration; it is reported in mm y^{-1} instead of
306 mm d^{-1} throughout the paper to enhance interpretability.

307 Our model belongs to the family of coupled soil moisture and biomass models developed for
308 other purposes^{61–63}. The key difference is that many earlier models treated biomass growth and
309 evapotranspiration as the same function scaled by a constant conversion factor, water use efficiency,
310 defined as water loss per unit carbon assimilation. Here, both processes depend on moisture, biomass,
311 and tree density, but they have different functional forms, so water use efficiency varies across
312 environments. This follows from the fact that shading can affect evapotranspiration and assimilation
313 differently (Fig. 1a). In addition, relative biomass growth declines with size through the logistic term,
314 whereas evapotranspiration remains proportional to biomass. These assumptions are both biologically
315 plausible and necessary for the mechanisms we study: if water use efficiency were constant across
316 shading levels, the trivial pattern where partial shade is beneficial but heavy shade is detrimental
317 could not arise.

318 Below, we discuss in more detail the two main mechanisms employed in this paper.

319 Canopy mechanism

320 Shading affects both plant growth, by reducing light availability and thus photosynthesis, and
321 transpiration, by lowering temperature and radiation levels, which helps retain soil moisture and
322 improve water availability for herbs. When the shading mechanism is “on”, the root mechanism is
323 disabled by setting $f_h(S, d) = 0$, implying a complete partitioning of the soil into two distinct niches,
324 the top available for herbs only, and deeper layers accessible to trees only.

325 Biomass growth is down-regulated by shading via $f_a(d)$, while evapotranspiration is down-regulated
326 via $f_e(d)$. The shading functions are $f_j(d) = (1 - d)^{\beta_j}$, where $j = \{a, e\}$. Figure 1a shows the
327 nonlinear decline of these functions with tree density. A necessary condition for facilitation is $\beta_e > \beta_a$;
328 assimilation is therefore less inhibited by shade than transpiration.

329 **Root mechanism**

330 Trees can influence herbs access to water in two ways: they can lift water from deeper layers into
331 the herbs rooting zone when surface soil is dry (facilitation), and they can uptake water from that
332 zone (competition). The combined effects of hydraulic lift and tree water uptake is described by the
333 function $f_r(S, d)$. When the root mechanism is “on”, the shading mechanism is disabled by setting
334 $f_a(d) = f_e(d) = 1$. The expression for the root function reads:

$$f_r(S, d) = d [\lambda_1 + \varphi \max(0, S - S_h) - \varphi \max(0, S - S_{fc})], \quad (2)$$

335 where the slope $\varphi = (\lambda_{fc} - \lambda_h)/(S_{fc} - S_h)$. For S smaller than the hygroscopic point S_h , the upper
336 soil is too dry for tree roots to uptake water, and hydraulic lift reaches its maximum ability to bring
337 water from deeper soil layers to the topsoil (λ_h). For S greater than the field capacity S_{fc} , trees cease
338 to benefit from increasing soil water content, and uptake water at a rate λ_{fc} . Between S_h and S_{fc} , the
339 root function varies linearly between λ_h and λ_{fc} . Regardless of soil water content, the root function
340 depends linearly on tree density d . Figure 1b shows the function f_r in the range $S_h < S < S_{fc}$, for
341 zero tree density ($d = 0$) and maximal tree density ($d = 1$).

342 **4.1 Numerical solutions**

343 Numerical analyses were performed with Python 3.12, using the libraries NumPy 2.0 and SciPy 1.13.
344 Steady-state solutions ($dB/dt = dS/dt = 0$) were obtained by finding the roots of the right-hand side of
345 Eqs. (1) with `scipy.optimize.fsolve`, using random starting estimates for the roots ($0.5 < B < 1.5 \text{ kg m}^{-2}$
346 and $0.5 < S < 0.6$). A root is accepted when $B > 0.01 \text{ kg m}^{-2}$ and $0 < S < 1$; if these criteria are
347 not met, a new set of random starting estimates is chosen. This procedure is repeated up to 10
348 times, after which the steady-state solutions are estimated by numerically integrating Eqs. (1) with
349 `scipy.integrate.solve_ivp` (stiff solver, default tolerances) up to a final time of 10 thousand days, and
350 the final configuration is taken as the steady-state solutions.

351 **4.2 Code Availability**

352 The code to run the model can be found in the following Zenodo repository
353 <https://doi.org/10.5281/zenodo.17641468>.

354 **4.3 Model Parameters**

355 The model variables and parameters are summarized in Table 1. The specific parameter values (or
356 their ranges) were chosen from typical values found in the literature.

Table 1: Variables and parameters with typical value ranges.

Variables			
Symbol	Units	Values	Description
B	g m^{-2}	0–1000	Herb biomass density
S	—	0–1	Relative soil water content
Parameters			
a	d^{-1}	0.05	Assimilation rate
β_a	—	1/3	Shading function exponent
β_e	—	4	Shading function exponent
k	g m^{-2}	1000	Carrying capacity
m	d^{-1}	0.01	Mortality rate
p	mm y^{-1}	0–600	Precipitation rate
e_0	$\text{mm d}^{-1}/\text{g m}^{-2}$	0.005	Max evapotranspiration rate per unit biomass density
q_{sat}	mm d^{-1}	800	Saturated hydraulic conductivity
γ	—	10	Deep infiltration exponent
n	—	0.4	Soil porosity
z_r	mm	300	Herb rooting depth
d	—	0–1	Woody plant density
S_h	—	0.3	Hygroscopic point
S_{fc}	—	0.6	Field capacity
λ_h	mm d^{-1}	–2	Max tree water provision
λ_{fc}	mm d^{-1}	10	Max tree water usage

Note. Variable B range derived from Mussery et al.⁶⁴. Variable S range and parameters q_{sat} , γ , n , z_r , S_h , S_{fc} derived from Rodriguez-Iturbe et al.⁶⁰. Parameter a derived from James and Drenovsky⁶⁵. The ratio between β_a and β_e is derived from Pons et al.⁶⁶. Parameter p range derived from Huang et al.⁶⁷. Parameter λ_{fc} is derived from Shiferaw et al.⁶⁸. Parameter e_0 is derived from Allen et al.⁶⁹; Garnier et al.⁷⁰.

5 Acknowledgments

We thank Barel Tsafon, Atay Mor, Santanu Das, Erez Feuer and Moshe Shachack for comments on earlier drafts. We thank Jonathan Friedman for useful discussion. Figure 1 utilized the images: oak by Levi, roots by wahab marhaban, grass by Jhonatan, all from the Noun Project (CC BY 3.0). This work was supported by the Center for Sustainability, and by the Research Center for Agriculture, Environment and Natural Resources, both of the Hebrew University of Jerusalem.

³⁶³ **6 Competing Interests**

³⁶⁴ The authors declare no competing interests.

³⁶⁵ **7 Author Contribution**

³⁶⁶ Conceptualization: O.H., Y.M., and N.D.; Analysis: O.H. and Y.M.; Funding acquisition: Y.M. and
³⁶⁷ N.D.; Supervision: Y.M. and N.D.; Visualization: O.H. and Y.M.; Writing—original draft: O.H.;
³⁶⁸ Writing—review and editing: Y.M. and N.D.

369 References

- 370 [1] Karina Winkler, Richard Fuchs, Mark Rounsevell, and Martin Herold. Global land use changes
371 are four times greater than previously estimated. *Nature Communications*, 12:2501, 05 2021. doi:
372 10.1038/s41467-021-22702-2.
- 373 [2] Lucio Biancari, Martín R. Aguiar, David J. Eldridge, Gastón R. Oñatibia, Yoann Le Bagousse-
374 Pinguet, Hugo Saiz, Nicolas Gross, Amy T. Austin, Victoria Ochoa, Beatriz Gozalo, et al.
375 Drivers of woody dominance across global drylands. *Science Advances*, 10(41), 10 2024. doi:
376 10.1126/sciadv.adn6007.
- 377 [3] Fernando T. Maestre, Manuel Delgado-Baquerizo, Thomas C. Jeffries, David J. Eldridge, Victoria
378 Ochoa, Beatriz Gozalo, José Luis Quero, Miguel García-Gómez, Antonio Gallardo, Werner
379 Ulrich, Matthew A. Bowker, Tulio Arredondo, Claudia Barraza-Zepeda, Donaldo Bran, Adriana
380 Florentino, Juan Gaitán, Julio R. Gutiérrez, Elisabeth Huber-Sannwald, Mohammad Jankju,
381 Rebecca L. Mau, Maria Miriti, Kamal Naseri, Abelardo Ospina, Ilan Stavi, Deli Wang, Natasha N.
382 Woods, Xia Yuan, Eli Zaady, and Brajesh K. Singh. Increasing aridity reduces soil microbial
383 diversity and abundance in global drylands. *Proceedings of the National Academy of Sciences*,
384 112(51):15684–15689, 12 2015. doi: 10.1073/pnas.1516684112.
- 385 [4] Amir Lewin, Gopal Murali, Shimon Rachmilevitch, and Uri Roll. Global evaluation of current
386 and future threats to drylands and their vertebrate biodiversity. *Nature Ecology & Evolution*, 8
387 (8):1448–1458, August 2024. ISSN 2397-334X. doi: 10.1038/s41559-024-02450-4.
- 388 [5] Xuezheng Zong, Xiaorui Tian, Xiaodong Liu, and Lifu Shu. Drought threat to terrestrial gross
389 primary production exacerbated by wildfires. *Communications Earth & Environment*, 5:225, 4
390 2024. doi: 10.1038/s43247-024-01406-7.
- 391 [6] Robert K. Shriver, Elise Pletcher, Franco Biondi, Alexandra K. Urza, and Peter J. Weisberg.
392 Long-term tree population growth can predict woody encroachment patterns. *Proceedings of the
393 National Academy of Sciences*, 122(18):e2424096122, 5 2025. doi: 10.1073/pnas.2424096122.
- 394 [7] Chi Chen, Taeyoung Park, Xuhui Wang, Shilong Piao, Bing Xu, Rajiv K. Chaturvedi, Richard
395 Fuchs, Victor Brovkin, Philippe Ciais, Rasmus Fensholt, Hans Tømmervik, Govindasamy Bala,
396 Zhihao Zhu, Ramakrishna R. Nemani, and Ranga B. Myneni. China and India lead in greening
397 of the world through land-use management. *Nature Sustainability*, 2(2):122–129, 2 2019. doi:
398 10.1038/s41893-019-0220-7.
- 399 [8] Clive G. Jones, John H. Lawton, and Moshe Shachak. Organisms as ecosystem engineers. *Oikos*,
400 69(3):373–386, 1994. URL <https://www.jstor.org/stable/3545850>.
- 401 [9] Milena Holmgren and Marten Scheffer. Strong facilitation in mild environments: The stress
402 gradient hypothesis revisited. *Journal of Ecology*, 98(6):1269–1275, 2010. ISSN 1365-2745. doi:
403 10.1111/j.1365-2745.2010.01709.x.
- 404 [10] C. J. Lortie, Alessandro Filazzola, Mike Westphal, and H. Scott Butterfield. Foundation plant
405 species provide resilience and microclimatic heterogeneity in drylands. *Scientific Reports*, 12
406 (18005), 2022. doi: 10.1038/s41598-022-22579-1. URL <https://www.nature.com/articles/s41598-022-22579-1>.
- 408 [11] Ying Fan, Gabriel M. Maherli, Erika G. Jobbág, Robert B. Jackson, and Clément O. Couvreur.
409 Hydrologic regulation of plant rooting depth. *Proceedings of the National Academy of Sciences*,
410 114(40):10572–10577, 2017. doi: 10.1073/pnas.1712381114.
- 411 [12] Iván Prieto, Cristina Armas, and Francisco I. Pugnaire. Water release through plant roots:
412 new insights into its consequences at the plant and ecosystem level. *New Phytologist*, 193

- 413 (4):830–841, 2012. doi: <https://doi.org/10.1111/j.1469-8137.2011.04039.x>. URL <https://onlinelibrary.wiley.com/doi/abs/10.1111/j.1469-8137.2011.04039.x>.
- 414
- 415 [13] Shenglan Sha, Gaochao Cai, Shurong Liu, and Mutez Ali Ahmed. Roots to the rescue: how plants
416 harness hydraulic redistribution to survive drought across contrasting soil textures. *Advanced
417 Biotechnology*, 2(43), 2024. doi: 10.1007/s44307-024-00050-8. URL <https://link.springer.com/article/10.1007/s44307-024-00050-8>.
- 416
- 417 [14] Justin Dohn, Fadiala Dembélé, Moussa Karembe, Aristides Moustakas, Kosiwa A. Amévor, and
418 Niall P. Hanan. Tree effects on grass growth in savannas: Competition, facilitation and the
419 stress-gradient hypothesis. *Journal of Ecology*, 101(1):202–209, 2013. ISSN 1365-2745. doi:
420 [10.1111/1365-2745.12010](https://doi.org/10.1111/1365-2745.12010).
- 421
- 422 [15] Qiang He, Mark D. Bertness, and Andrew H. Altieri. Global shifts towards positive species
423 interactions with increasing environmental stress. *Ecology Letters*, 16(5):695–706, 2013. ISSN
424 1461-0248. doi: [10.1111/ele.12080](https://doi.org/10.1111/ele.12080).
- 425
- 426 [16] Amy E. Adams, Elizabeth M. Besozzi, Golya Shahrokhi, and Michael A. Patten. A case for
427 associational resistance: Apparent support for the stress gradient hypothesis varies with study
428 system. *Ecology Letters*, 25(1):202–217, 2022. ISSN 1461-0248. doi: [10.1111/ele.13917](https://doi.org/10.1111/ele.13917).
- 429
- 430 [17] Fernando T. Maestre, Fernando Valladares, and James F. Reynolds. Is the change of plant–plant
431 interactions with abiotic stress predictable? A meta-analysis of field results in arid environments.
Journal of Ecology, 93(4):748–757, 2005. ISSN 1365-2745. doi: [10.1111/j.1365-2745.2005.01017.x](https://doi.org/10.1111/j.1365-2745.2005.01017.x).
- 432
- 433 [18] Mark Bertness and Scott Shumway. Competition and facilitation in marsh plants. *The American
naturalist*, 142:718–24, 11 1993. doi: [10.1086/285567](https://doi.org/10.1086/285567).
- 434
- 435 [19] Mark D. Bertness and Ragan Callaway. Positive interactions in communities. *Trends in Ecology
& Evolution*, 9(5):191–193, May 1994. ISSN 0169-5347. doi: [10.1016/0169-5347\(94\)90088-4](https://doi.org/10.1016/0169-5347(94)90088-4).
- 436
- 437 [20] Milena Holmgren, Marten Scheffer, and Michael A. Huston. The Interplay of Facilitation and
438 Competition in Plant Communities. *Ecology*, 78(7):1966–1975, 1997. ISSN 0012-9658. doi:
439 [10.2307/2265937](https://doi.org/10.2307/2265937).
- 440
- 441 [21] Ragan M. Callaway and Lawrence R. Walker. Competition and facilitation: A synthetic approach
442 to interactions in plant communities. *Ecology*, 78(7):1958–1965, 1997. doi: [https://doi.org/10.1890/0012-9658\(1997\)078\[1958:CAFASA\]2.0.CO;2](https://doi.org/10.1890/0012-9658(1997)078[1958:CAFASA]2.0.CO;2). URL <https://esajournals.onlinelibrary.wiley.com/doi/abs/10.1890/0012-9658%281997%29078%5B1958%3ACAFASA%5D2.0.CO%3B2>.
- 442
- 443
- 444 [22] Rob W Brooker and Terry V Callaghan. The balance between positive and negative plant
445 interactions and its relationship to environmental gradients: a model. *Oikos*, pages 196–207,
446 1998.
- 447
- 448 [23] Mark D. Bertness, Lohengrin A. Cavieres, C.J. Lortie, and Ragan M. Callaway. Positive
449 interactions and interdependence in communities. *Trends in Ecology & Evolution*, 39:
450 1014–1023, 2024. doi: [10.1016/j.tree.2024.09.003](https://doi.org/10.1016/j.tree.2024.09.003). URL [https://www.cell.com/trends/ecology-evolution/fulltext/S0169-5347\(24\)00224-6](https://www.cell.com/trends/ecology-evolution/fulltext/S0169-5347(24)00224-6).
- 451
- 452 [24] Ruichang Zhang and Katja Tielbörger. Density-dependence tips the change of plant–plant
453 interactions under environmental stress. *Nature Communications*, 11(1):2532, 2020. doi:
454 [10.1038/s41467-020-16286-6](https://doi.org/10.1038/s41467-020-16286-6). URL <https://www.nature.com/articles/s41467-020-16286-6>.

- 454 [25] Ragan M. Callaway, R. W. Brooker, Philippe Choler, Zaal Kikvidze, Christopher J. Lortie,
455 Richard Michalet, Leonardo Paolini, Francisco I. Pugnaire, Beth Newingham, Erik T. Aschehoug,
456 Cristina Armas, David Kikodze, and Bradley J. Cook. Positive interactions among alpine
457 plants increase with stress. *Nature*, 417:844–848, 2002. doi: 10.1038/nature00812. URL
458 <https://www.nature.com/articles/nature00812>.
- 459 [26] J.m.j Travis, R.w Brooker, and C Dytham. The interplay of positive and negative species
460 interactions across an environmental gradient: Insights from an individual-based simulation
461 model. *Biology Letters*, 1(1):5–8, March 2005. doi: 10.1098/rsbl.2004.0236.
- 462 [27] Sa Xiao, Richard Michalet, Gang Wang, and Shu-Yan Chen. The interplay between species'
463 positive and negative interactions shapes the community biomass–species richness relationship.
464 *Oikos*, 118(9):1343–1348, 2009. ISSN 1600-0706. doi: 10.1111/j.1600-0706.2009.17588.x.
- 465 [28] Richard Michalet. Highlighting the multiple drivers of change in interactions along stress gradients.
466 *New Phytologist*, 173(1):3–6, 2007. doi: <https://doi.org/10.1111/j.1469-8137.2006.01949.x>. URL
467 <https://nph.onlinelibrary.wiley.com/doi/abs/10.1111/j.1469-8137.2006.01949.x>.
- 468 [29] Fernando T. Maestre, Ragan M. Callaway, Fernando Valladares, and Christopher J. Lortie.
469 Refining the stress-gradient hypothesis for competition and facilitation in plant communities.
470 *Journal of Ecology*, 97(2):199–205, 2009. ISSN 1365-2745. doi: 10.1111/j.1365-2745.2008.01476.x.
- 471 [30] Dan Falkinson and Katja Tielbörger. What does the stress-gradient hypothesis predict?
472 Resolving the discrepancies. *Oikos*, 119:1546–1552, May 2010. doi: 10.1111/j.1600-0706.2010.
473 18375.x.
- 474 [31] Santiago Soliveres, Christian Smit, and Fernando T. Maestre. Moving forward on facilitation
475 research: response to changing environments and effects on the diversity, functioning and evolution
476 of plant communities. *Biological Reviews*, 90(1):297–313, 2015. doi: <https://doi.org/10.1111/brv.12110>. URL
477 <https://onlinelibrary.wiley.com/doi/abs/10.1111/brv.12110>.
- 478 [32] Robert H. MacArthur. *Geographical Ecology: Patterns in the Distribution of Species*. Princeton
479 University Press, Princeton, NJ, 1972. ISBN 9780691023823.
- 480 [33] David Tilman. *Resource Competition and Community Structure*, volume 17 of *Monographs in
481 Population Biology*. Princeton University Press, Princeton, NJ, 1982. ISBN 9780691083025.
- 482 [34] Andrew D. Letten, Po-Ju Ke, and Tadashi Fukami. Linking modern coexistence theory and
483 contemporary niche theory. *Ecological Monographs*, 87(2):161–177, 2017. doi: <https://doi.org/10.1002/ecm.1242>. URL
484 <https://esajournals.onlinelibrary.wiley.com/doi/abs/10.1002/ecm.1242>.
- 485 [35] Thomas Koffel, Tanguy Daufresne, and Christopher A. Klausmeier. From competition to
486 facilitation and mutualism: a general theory of the niche. *Ecological Monographs*, 91(3):e01458,
487 2021. doi: <https://doi.org/10.1002/ecm.1458>. URL
488 <https://esajournals.onlinelibrary.wiley.com/doi/abs/10.1002/ecm.1458>.
- 489 [36] Ciro Cabal, Gabriel A. Maciel, and Ricardo Martinez-Garcia. Plant antagonistic facilitation across
490 environmental gradients: A soil-resource ecosystem engineering model. *New Phytologist*, 244(2):
491 670–682, October 2024. ISSN 0028-646X, 1469-8137. doi: 10.1111/nph.20053.
- 492 [37] Rubén Díaz-Sierra, Max Rietkerk, Mart Verwijmeren, and Mara Baudena. Facilitation and
493 competition deconstructed: A mechanistic modelling approach to the stress gradient hypothesis
494 applied to drylands. *Scientific Reports*, 14(1):2205, January 2024. ISSN 2045-2322. doi:
495 10.1038/s41598-024-52447-z.

- 497 [38] Antonio I. Arroyo, Yolanda Pueyo, Hugo Saiz, and Concepción L. Alados. Plant–plant interactions
498 as a mechanism structuring plant diversity in a mediterranean semi-arid ecosystem. *Ecology
499 and Evolution*, 5(22):5305–5317, 2015. doi: <https://doi.org/10.1002/ece3.1770>. URL <https://onlinelibrary.wiley.com/doi/abs/10.1002/ece3.1770>.
- 500 [39] Bradley J. Butterfield, John B. Bradford, Cristina Armas, Ivan Prieto, and Francisco I. Pugnaire.
501 Does the stress-gradient hypothesis hold water? disentangling spatial and temporal variation in
502 plant effects on soil moisture in dryland systems. *Functional Ecology*, 30(1):10–19, 2016. doi:
503 [10.1111/1365-2435.12592](https://doi.org/10.1111/1365-2435.12592). URL <https://besjournals.onlinelibrary.wiley.com/doi/full/10.1111/1365-2435.12592>.
- 506 [40] Michal Gruntman, Dorothee Groß, Maria Májeková, and Katja Tielbörger. Decision-making
507 in plants under competition. *Nature Communications*, 8:2235, 2017. doi: [10.1038/s41467-017-02147-2](https://doi.org/10.1038/s41467-017-02147-2). URL <https://www.nature.com/articles/s41467-017-02147-2>.
- 509 [41] Anu Eskelinen, W. Stanley Harpole, Maria-Theresa Jessen, Risto Virtanen, and Yann Hautier.
510 Light competition drives herbivore and nutrient effects on plant diversity. *Nature*, 611:301–
511 305, 2022. doi: [10.1038/s41586-022-05383-9](https://doi.org/10.1038/s41586-022-05383-9). URL <https://www.nature.com/articles/s41586-022-05383-9>.
- 513 [42] Liting Zheng, Kathryn E. Barry, Nathaly R. Guerrero-Ramírez, Dylan Craven, Peter B. Reich,
514 Kris Verheyen, Michael Scherer-Lorenzen, Nico Eisenhauer, Nadia Barsoum, Jürgen Bauhus,
515 Helge Bruelheide, Jeannine Cavender-Bares, Jiri Dolezal, Harald Auge, Marina V. Fagundes,
516 Olga Ferlian, Sebastian Fiedler, David I. Forrester, Gislene Ganade, Tobias Gebauer, Josephine
517 Haase, Peter Hajek, Andy Hector, Bruno Héault, and Yann Hautier. Effects of plant diversity
518 on productivity strengthen over time due to trait-dependent shifts in species overyielding. *Nature
519 Communications*, 15:2078, 2024. doi: [10.1038/s41467-024-46355-z](https://doi.org/10.1038/s41467-024-46355-z). URL <https://www.nature.com/articles/s41467-024-46355-z>.
- 521 [43] Rongxu Shan, Ganxin Feng, Yuwei Lin, and Zilong Ma. Temporal stability of forest productivity
522 declines over stand age at multiple spatial scales. *Nature Communications*, 16:2745, 2025. doi:
523 [10.1038/s41467-025-57984-3](https://doi.org/10.1038/s41467-025-57984-3). URL <https://www.nature.com/articles/s41467-025-57984-3>.
- 524 [44] John E. Cantlon. Vegetation and microclimates on north and south slopes of cusetunk
525 mountain, new jersey. *Ecological Monographs*, 23(3):241–270, 1953. doi: [10.2307/1943593](https://doi.org/10.2307/1943593). URL
526 <https://esajournals.onlinelibrary.wiley.com/doi/10.2307/1943593>.
- 527 [45] Gaofei Yin, Jiangliu Xie, Dujuan Ma, Qiaoyun Xie, Aleixandre Verger, Adrià Descals, Iolanda
528 Filella, and Josep Peñuelas. Aspect matters: Unraveling microclimate impacts on mountain
529 greenness and greening. *Geophysical Research Letters*, 50(24):e2023GL105879, 2023. doi: [10.1029/2023GL105879](https://doi.org/10.1029/2023GL105879). URL <https://agupubs.onlinelibrary.wiley.com/doi/full/10.1029/2023GL105879>.
- 532 [46] J. Widmer, B. Christ, J. Grenz, and L. Norgrove. Agrivoltaics, a promising new tool for
533 electricity and food production: A systematic review. *Renewable and Sustainable Energy Reviews*,
534 192:114277, 2024. ISSN 1364-0321. doi: <https://doi.org/10.1016/j.rser.2023.114277>. URL
535 <https://www.sciencedirect.com/science/article/pii/S1364032123011358>.
- 536 [47] Katia Tielbörger and Ronen Kadmon. Temporal environmental variation tips the balance between
537 facilitation and interference in desert plants. *Ecology*, 81:1544–1553, 06 2000. doi: [10.2307/177305](https://doi.org/10.2307/177305).
- 538 [48] Aristides Moustakas, William E. Kunin, Tom C. Cameron, and Mahesh Sankaran. Facilitation
539 or competition? tree effects on grass biomass across a precipitation gradient. *PLoS ONE*, 8(2):
540 e57025, 2013. doi: [10.1371/journal.pone.0057025](https://doi.org/10.1371/journal.pone.0057025).

- 541 [49] Carin J. Ragland, Kevin Y. Shih, and José R. Dinneny. Choreographing root architecture and
542 rhizosphere interactions through synthetic biology. *Nature Communications*, 15(1370), 2024. doi:
543 10.1038/s41467-024-45272-5. URL <https://www.nature.com/articles/s41467-024-45272-5>.
- 544 [50] David Ward, Kerstin Wiegand, and Stephan Getzin. Walter's two-layer hypothesis revisited:
545 Back to the roots! *Oecologia*, 172(3):617–630, July 2013. ISSN 1432-1939. doi: 10.1007/
546 s00442-012-2538-y.
- 547 [51] José M. Grünzweig, Hans J. De Boeck, Ana Rey, Maria J. Santos, Ori Adam, Michael
548 Bahn, Jayne Belnap, Gaby Deckmyn, Stefan C. Dekker, Omar Flores, Daniel Gliksman, David
549 Helman, Kevin R. Hultine, Lingli Liu, Ehud Meron, Yaron Michael, Efrat Sheffer, Heather L.
550 Throop, Omer Tzuk, and Dan Yakir. Dryland mechanisms could widely control ecosystem
551 functioning in a drier and warmer world. *Nature Ecology & Evolution*, 6:1064–1076, 2022. doi:
552 10.1038/s41559-022-01779-y. URL <https://www.nature.com/articles/s41559-022-01779-y>.
- 553 [52] Jasper M. C. Denissen, Adriaan J. Teuling, Andy J. Pitman, Sujan Koirala, Mirco Migliavacca,
554 Wantong Li, Markus Reichstein, Alexander J. Winkler, Chunhui Zhan, and Rene Orth.
555 Widespread shift from ecosystem energy to water limitation with climate change. *Nature Climate
556 Change*, 12:677–684, 2022. doi: 10.1038/s41558-022-01403-8.
- 557 [53] Melinda D. Smith, Kate D. Wilkins, Martin C. Holdrege, Xiaoan Zuo, and et al. Extreme drought
558 impacts have been underestimated in grasslands and shrublands globally. *Proceedings of the
559 National Academy of Sciences*, 121(4):e2309881120, 2024. doi: 10.1073/pnas.2309881120. URL
560 <https://www.pnas.org/doi/10.1073/pnas.2309881120>.
- 561 [54] Lorenzo Rosa and Matteo Sangiorgio. Global water gaps under future warming levels. *Nature
562 Communications*, 16(1):1192, jan 2025. ISSN 2041-1723. doi: 10.1038/s41467-025-56517-2. URL
563 <https://doi.org/10.1038/s41467-025-56517-2>. Open access.
- 564 [55] Ignacio Rodríguez-Iturbe and Amilcare Porporato. *Ecohydrology of Water-Controlled Ecosystems:
565 Soil Moisture and Plant Dynamics*. Cambridge University Press, January 2004. ISBN 978-0-521-
566 81943-5. doi: 10.1017/CBO9780511535727.
- 567 [56] Andrew J. Guswa, M. A. Celia, and I. Rodriguez-Iturbe. Models of soil moisture dynamics in
568 ecohydrology: A comparative study. *Water Resources Research*, 38(9):5–15–15, 2002. ISSN
569 1944-7973. doi: 10.1029/2001WR000826.
- 570 [57] Thomas L. Powell, David R. Galbraith, Bradley O. Christoffersen, Anna Harper, Hewley M. A.
571 Imbuzeiro, Lucy Rowland, Samuel Almeida, Paulo M. Brando, Antonio Carlos Lola da Costa, et al.
572 Confronting model predictions of carbon fluxes with measurements of amazon forests subjected
573 to experimental drought. *New Phytologist*, 200(2):350–365, 2013. doi: 10.1111/nph.12390. URL
574 <https://nph.onlinelibrary.wiley.com/doi/10.1111/nph.12390>.
- 575 [58] Jean V. Wilkening, Xue Feng, Todd E. Dawson, and Sally E. Thompson. Different roads,
576 same destination: The shared future of plant ecophysiology and ecohydrology. *Plant, Cell &
577 Environment*, 47(9):3447–3465, 2024. doi: 10.1111/pce.14937. URL <https://onlinelibrary.wiley.com/doi/10.1111/pce.14937>.
- 579 [59] Roger B. Clapp and George M. Hornberger. Empirical equations for some soil hydraulic properties.
580 *Water Resources Research*, 14(4):601–604, 1978. doi: 10.1029/WR014i004p00601.
- 581 [60] I. Rodriguez-Iturbe, A. Porporato, F. Laio, and L. Ridolfi. Plants in water-controlled ecosystems:
582 Active role in hydrologic processes and response to water stress: I. Scope and general outline.
583 *Advances in Water Resources*, 24(7):695–705, 2001. ISSN 0309-1708. doi: 10.1016/S0309-1708(01)
584 00004-5.

- 585 [61] Christopher A Klausmeier. Regular and irregular patterns in semiarid vegetation. *Science*, 284
586 (5421):1826–1828, 1999.
- 587 [62] Erez Gilad, Jost Von Hardenberg, Antonello Provenzale, Moshe Shachak, and Ehud Meron.
588 Ecosystem engineers: from pattern formation to habitat creation. *Physical Review Letters*, 93
589 (9):098105, 2004.
- 590 [63] Benjamin E Schaffer, Jan M Nordbotten, and Ignacio Rodriguez-Iturbe. Plant biomass and soil
591 moisture dynamics: Analytical results. *Proceedings of the Royal Society A: Mathematical, Physical
592 and Engineering Sciences*, 471(2183):20150179, 2015.
- 593 [64] Amir Mussery, David Helman, Stefan Leu, and Arie Budovsky. Modeling herbaceous productivity
594 considering tree-grass interactions in drylands savannah: The case study of yatir farm in the negev
595 drylands. *Journal of Arid Environments*, 124:160–164, 2016. doi: 10.1016/j.jaridenv.2015.08.013.
- 596 [65] Jeremy J James and Rebecca E Drenovsky. A basis for relative growth rate differences between
597 native and invasive forb seedlings. *Rangeland ecology & management*, 60(4):395–400, 2007.
- 598 [66] Thijs L. Pons, Wilco Jordi, and Daan Kuiper. Acclimation of plants to light gradients in
599 leaf canopies: evidence for a possible role for cytokinins transported in the transpiration
600 stream. *Journal of Experimental Botany*, 52(360):1563–1574, 07 2001. ISSN 0022-0957. doi:
601 10.1093/jexbot/52.360.1563. URL <https://doi.org/10.1093/jexbot/52.360.1563>.
- 602 [67] Jianping Huang, Haipeng Yu, Aiguo Dai, Yun Wei, and Litai Kang. Drylands face potential threat
603 under 2 c global warming target. *Nature Climate Change*, 7(6):417–422, 2017.
- 604 [68] Hailu Shiferaw, Tena Alamirew, Sebinasi Dzikiti, Woldeamlak Bewket, Gete Zeleke, and Urs
605 Schaffner. Water use of *prosopis juliflora* and its impacts on catchment water budget and
606 rural livelihoods in afar region, ethiopia. *Scientific Reports*, 11(2688), 2021. doi: 10.1038/
607 s41598-021-81776-6. URL <https://www.nature.com/articles/s41598-021-81776-6>.
- 608 [69] Richard G Allen, Luis S Pereira, Dirk Raes, Martin Smith, et al. Crop evapotranspiration-
609 guidelines for computing crop water requirements-fao irrigation and drainage paper 56. *Fao, Rome*, 300(9):D05109, 1998.
- 610 [70] Eric Garnier, Marie-Laure Navas, and Karl Grigulis. *Plant functional diversity: organism traits,
611 community structure, and ecosystem properties*. Oxford University Press, 2016.

613

Supplementary Information

614

S1 Role of carrying capacity in the SGH patterns

615 We explore here the model results for each of the two mechanisms in the case where the logistic growth
 616 term is rendered inactive. This is achieved by taking the carrying capacity $k \rightarrow \infty$, which makes
 617 $f_k(B) = (1 - B/k) \rightarrow 1$. We can now find analytical expressions for the steady-state solutions of the
 618 model described in Equations (1) in the main paper. The nontrivial ($B \neq 0$) steady-state solutions
 619 (B^*, S^*) read:

$$S^* = \frac{m}{a f_a(d)} \quad (\text{S1a})$$

$$B^* = \frac{p - f_r(S^*, d) - q_s(S^*)^\gamma}{e_0 f_e(d) S^*} \quad (\text{S1b})$$

620

621 These solutions are a typical instance of the R-star rule¹ and from them we can express two important
 622 features:

- 623 1. The steady-state resource level S^* (generally called R^* in consumer-resource modeling, therefore
 624 the name of the rule) is independent of the resource supply rate, p .
- 625 2. The nontrivial ($B \neq 0$) steady-state consumer level B^* is linear in the resource input rate, p .

626 Figure S1 shows the steady-state biomass B^* (top panels) and relative soil water content S^* (bottom
 627 panels). The left and right columns correspond to the shading mechanism and the root mechanism,
 628 respectively. A careful examination of the steady-state solutions (S1) teaches us that:

- 629 • **For the shading mechanism,** $0 \leq f_e(d) < f_a(d) < 1$ for any $d > 0$ (see inset in Fig. S1c). From
 630 these facts it follows that the linear function for the positive tree-density solution ($B^*(p, d > 0)$)
 631 has a higher slope and a lower intercept² than the no-tree solution ($B^*(p, d = 0)$). Because of its
 632 lower intercept, the positive density solution surpasses the zero-tree density solution from below
 633 (lower B). This means that eliminating the logistic growth term from the model **reverses the**
 634 **order of the transition** described by the SGH: we have competition for p below the transition
 635 point, and facilitation for p above that point. Furthermore, for the parameter values we used
 636 here, the transition point occurs at extremely low values of p and B . Looking from ‘farther
 637 away’, the interactions appear facilitative for most of the precipitation gradient (Fig. S1a).
- 638 • **For the root mechanism,** two straight-line solutions B^* always have the same slope, regardless
 639 of their d value, and therefore never intersect. The root mechanism can be either facilitative or
 640 competitive, depending on the soil water content (see inset in Fig. S1d). Figure S1b shows a
 641 scenario where the interaction is always facilitative. By changing the model parameters m, a, d
 642 (see Eq. S1a), one can also find higher soil water content levels that always yield competitive
 643 interactions.

²Slope σ : for $d = 0$ the slope is $\sigma_0 = a/(e_0 m)$, whereas for $d > 0$ it is $\sigma_d = \sigma_0 \cdot (f_a(d)/f_e(d))$. Since $f_a(d) > f_e(d)$, we have that $\sigma_d > \sigma_0$.

Intercept ω : for $d = 0$ the intercept is $\omega_0 = -(q_s/e_d)(m/a)^{\gamma-1}$, whereas for $d > 0$ it is $\omega_d = \omega_0(1/f_e(d))(1/f_a^{\gamma-1}(d))$. Since $f_a(d), f_e(d) < 0$ and $\gamma > 2$, we have that each of the parenthesis in the expression for ω_d is greater than 1, and therefore $\omega_d < \omega_0$ (remember the minus sign in ω_0).

644 The arguments above demonstrate that, whenever tree density is constant, the **introduction of an**
 645 **additional growth-limiting factor** that strengthens with increasing precipitation is a **necessary**
 646 **condition** for the emergence of the transition described by the SGH.

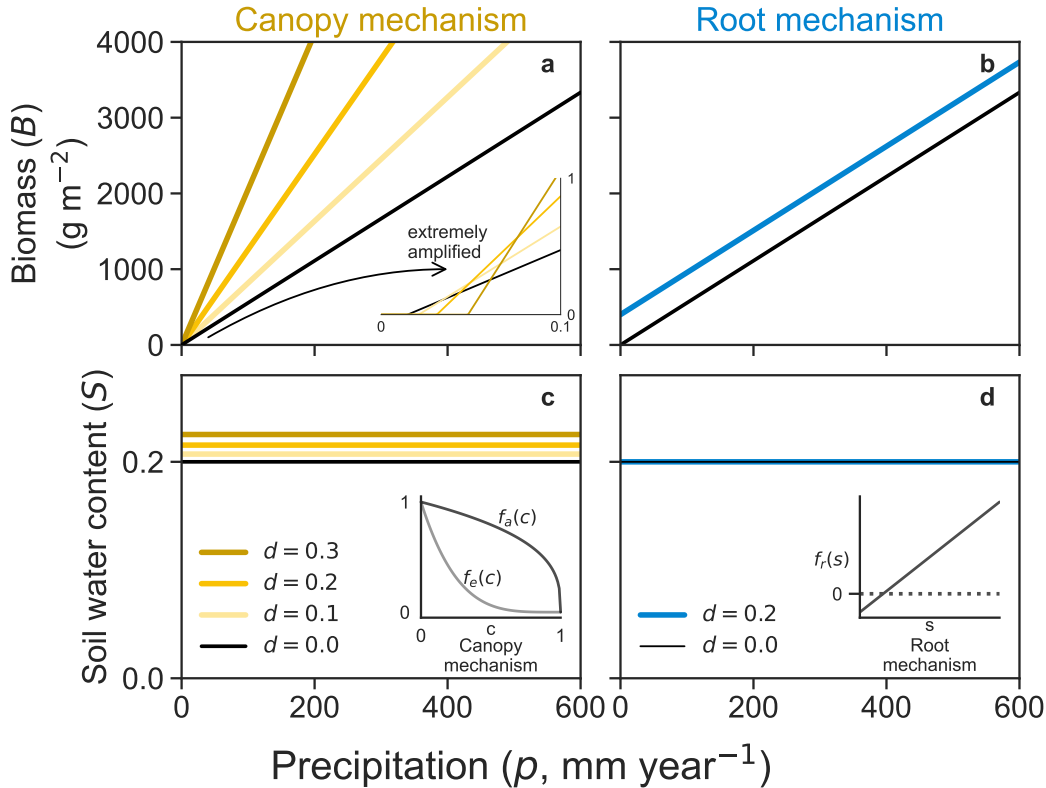


Figure S1: Steady-state biomass (panels a,b) and soil water content (panels c,d) solutions as functions of precipitation. The left column corresponds to the shading mechanism, and the right column corresponds to the root mechanism. The inset in panel a shows an extreme amplification in p and B of the solutions, emphasizing the intersection points between the no-tree solution ($d = 0$) and the other solutions with $d > 0$. The insets in panels c and d are provided as reminders of the relevant functions of each mechanism.

647 S2 Interaction intensity

648 As a rule, trees facilitate herb growth when their density is low and the system is under water stress
 649 (low p). Competition over water arises at high tree density values and under low water stress. Focusing
 650 on the canopy mechanism, Figure S2 shows that in the (p, d) parameter space, the boundary between
 651 facilitation and competition (solid black curve) follows a negative relation: as precipitation increases,
 652 a lower tree density is sufficient to shift the balance from facilitation to competition. This border is
 653 the same for both interaction intensities definitions, since zero interaction intensity means that the
 654 biomass solution with tree density (B_T) equals the biomass solution with no tree density (B_0). The
 655 area hatched in black at the top of both panels, where tree density is very high, indicates the region
 656 in the parameter space where there are only trivial ($B = 0$) vegetated solutions.

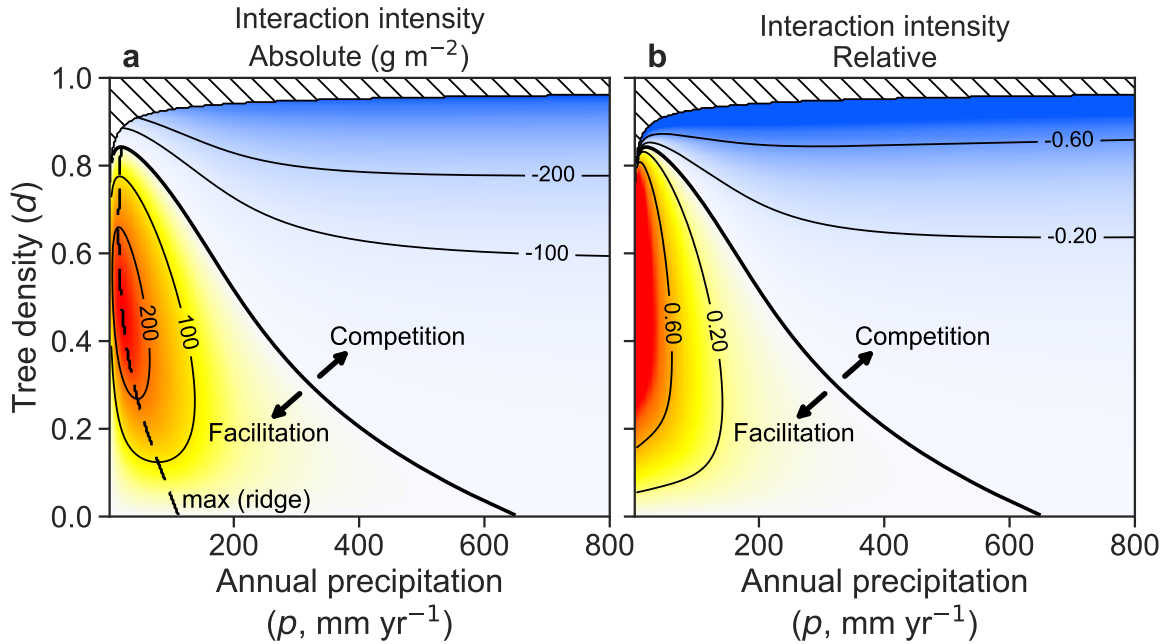


Figure S2: Interaction intensity varies jointly with precipitation and tree density. Interaction intensity in the canopy submodel is shown as a function of annual precipitation (p) and tree density (d), measured as (left) the absolute difference in herb biomass, $B_T - B_0$, and (right) the relative log response ratio, $\ln(B_T/B_0)$, where B_0 and B_T denote herb biomass in the absence and presence of trees, respectively. Purple shades indicate facilitation (positive values) and orange shades indicate competition (negative values). Both metrics reveal a transition (black line) from facilitation at low rainfall and tree density to competition at high rainfall and tree density. The dashed black line on the left panel indicates the locus of maximum facilitation for a fixed tree density value [$\frac{\partial}{\partial p}(\text{int. intensity}) = 0$], for the absolute interaction intensity.

As shown in Fig. 3a, we can get unimodal curves when using the absolute interaction intensity. The dashed black curve in Fig. S2a shows the location of the local maxima in the (p, d) parameter space. To the left of this curve, the interaction intensity is positive and increases with precipitation. Once we cross this curve (from left to right), interaction intensity is still positive, but it decreases with precipitation. This ridge-like curve disappears when we use the relative interaction intensity instead: there is only monotonic decrease with precipitation.

S3 A deeper look into the model

In order to find useful ways of thinking about the model, we perform a non-dimensionalization of the equations. For our purposes, it makes more sense to describe the second equation as the rate of change of absolute soil water content $W = nz_r S$, instead of the equivalent $nz_r dS/dt$ as shown in Eq. (1). Since the active soil layer nz_r has length dimension (z_r is the depth of the herb rooting zone, while the porosity n is non-dimensional), absolute soil water content W is also a length (it is commonly called soil water depth). Finally, we note that 1 mm of water is equivalent to 1 L m^{-2} , so reporting W as

length is the same as volume per unit area. The full model equations now read:

$$\frac{dB}{dt} = a f_a(d) \left(1 - \frac{B}{k}\right) B S - m B \quad (\text{S2a})$$

$$\frac{dW}{dt} = p - q_s S^\gamma - e_0 f_e(d) B S - f_r(S, d). \quad (\text{S2b})$$

671

672 The independent and dependent variables of this dynamical system have the following dimensions:

Quantity	symbol	dimension	units
Biomass density	B	density ρ	kg m^{-2}
Absolute soil water content	W	length L	mm
Time	t	time T	day

673 Accounting for all the model parameters that have dimensions, we have eight: $a, k, m, (nz_r), p, q_s, e_0, \lambda$.
 674 (Here we treat nz_r as a single parameter.) The parameter λ appears inside the function $f_r(S, d)$. All of
 675 these parameters have dimensions that derive from the three basic ones shown in the table. According
 676 to Buckingham's II Theorem, when performing non-dimensionalization of the equations, the number of
 677 independent dimensionless groups is equal to the number of dimensional parameters minus the number
 678 of fundamental dimensions. Since we have 8 dimensional parameters and 3 fundamental dimensions
 679 (biomass density, length, and time), we obtain $8 - 3 = 5$. In simple terms, although the model contains
 680 eight dimensional parameters, its behavior can be fully captured by just five independent dimensionless
 681 combinations.

682 We start now the non-dimensionalization process by defining the following new non-dimensional
 683 variables:

$$\text{non-dimensional biomass} \quad \tilde{b} = B/\xi_1 \quad (\text{S3a})$$

$$\text{non-dimensional time} \quad \tilde{t} = \frac{t}{\xi_2}. \quad (\text{S3b})$$

$$\text{non-dimensional water} \quad S = \frac{W}{\xi_3}. \quad (\text{S3c})$$

684

685 We have many choices for ξ_1, ξ_2, ξ_3 . A suitable choice here is

$$\xi_1 = \frac{1}{e_0/a} \quad (\text{S4a})$$

$$\xi_2 = \frac{1}{a} \quad (\text{S4b})$$

$$\xi_3 = nz_r. \quad (\text{S4c})$$

686

687 Substituting Eqs. (S3) and (S4) into Eqs. (S2) yields the non-dimensional dynamical system:

$$\frac{d\tilde{b}}{d\tilde{t}} = f_a(d) \left(1 - \frac{\tilde{b}}{\tilde{k}}\right) \tilde{b} S - \tilde{m} \tilde{b} \quad (\text{S5a})$$

$$\frac{dS}{d\tilde{t}} = \tilde{p} - \tilde{q}_s S^\gamma - f_e(d) \tilde{b} S - \tilde{f}_r(S, d). \quad (\text{S5b})$$

688 As we can see, this choice of ξ_1, ξ_2, ξ_3 leaves us a non-dimensional system, where every single variable,
 689 parameter, term or function is dimensionless. For this specific choice of ξ scaling factors, we have a
 690 system with unity growth rate and unity maximum evapotranspiration rate.

691 The non-dimensional parameters (Π parameters) for the equations above are:

$$\text{non-dimensional herb growth rate , } \Pi_1 \quad \tilde{m} = \frac{m}{a} \quad (\text{S6a})$$

$$\text{non-dimensional carrying capacity , } \Pi_2 \quad \tilde{k} = (e_0/a)k \quad (\text{S6b})$$

$$\text{non-dimensional precipitation rate , } \Pi_3 \quad \tilde{p} = \frac{p}{anz_r} \quad (\text{S6c})$$

$$\text{non-dimensional sat. hyd. cond. , } \Pi_4 \quad \tilde{q}_s = \frac{q_s}{anz_r} \quad (\text{S6d})$$

$$\text{non-dimensional tree-root hydraulic rate , } \Pi_5 \quad \tilde{\lambda} = \frac{\lambda}{anz_r} \quad (\text{S6e})$$

692

693 This exercise is instrumental in shedding light on the impact of various model parameters on its
 694 behavior:

- 695 • The active soil layer nz_r (mm), where n is soil porosity (dimensionless) and z_r is the rooting
 696 depth of herbs (mm), sets the maximum volume of water that can be stored and made available
 697 to herbs. As Eqs. (1) indicate, nz_r can only impact the transient dynamics of (B, S) , never their
 698 steady-state solutions. Of course, due to the third conversion in Eq. (S3), nz_r rescales S into
 699 $W = nz_r S$.
- 700 • The denominator anz_r represents a characteristic water throughput, where a sets the
 701 characteristic timescale and nz_r is the volume of water per unit area ($1 \text{ mm} = 1 \text{ L mm}^{-2}$). It sets
 702 the scale for precipitation, drainage, and root uptake/uplift ($\tilde{p}, \tilde{q}_s, \tilde{\lambda}$): higher values correspond
 703 to processes faster than the characteristic resource throughput in the system.
- 704 • The ratio e_0/a naturally emerges as a water-use efficiency, converting herb water uptake into
 705 biomass production. In fact, when tree density is zero ($d = 0$) and herb biomass is low (so that
 706 $1 - \tilde{b}/\tilde{k} \approx 1$), the evapotranspiration loss term in Eq. (S5b) is identical to the biomass growth
 707 term in Eq. (S5a). This symmetry highlights the direct coupling of growth and water loss. The
 708 conversion dictated by (S3a) means that whatever the non-dimensional steady state \tilde{b} one gets
 709 by solving Eqs. (S5), we divide it by the water-use efficiency e_0/a to get the dimensional biomass
 710 B .
- 711 • The typical growth timescale $1/a$ acts as a fundamental clock for all other remaining parameters
 712 (see (S6)).
- 713 • \tilde{k} shows how the dimensional carrying capacity k is rescaled by water-use efficiency e_0/a . A
 714 system with a large k but low water-use efficiency is effectively constrained, while high water-use
 715 efficiency inflates the effective carrying capacity.

716 S4 Transient dynamics

717 The typical timescale for the dynamics of herb biomass (B) is comparable to the length of the growing
 718 season used in this study, 180 days. Figure S3 shows the time dynamics (left column) and phase space
 719 (right column) for three precipitation levels ($p = \{150, 300, 600\} \text{ mm year}^{-1}$) and three tree conditions:
 720 no tree ($d = 0$, top row), shading mechanism ($d = 0.3$, middle row), and root mechanism ($d = 0.3$,

bottom row). Linear stability analysis of the numerically found steady-state solutions (hollow circles) reveals them to be stable nodes (real and negative eigenvalues).

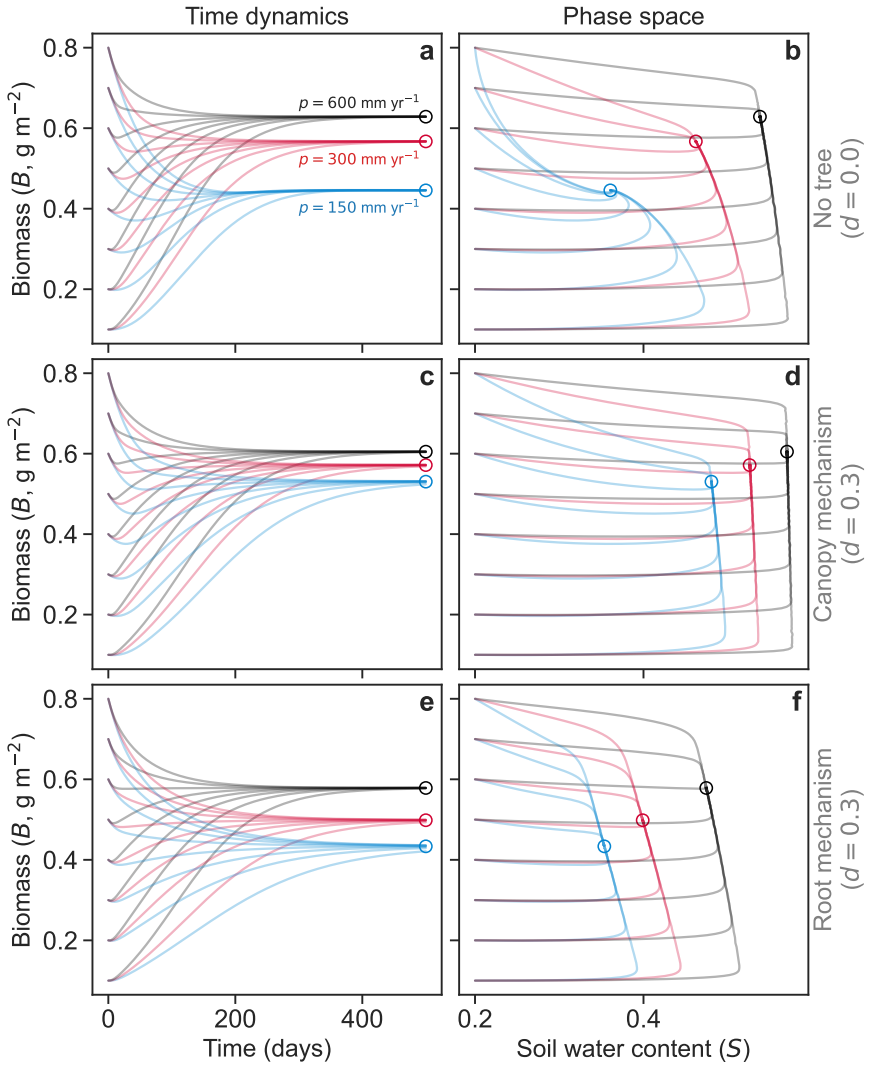


Figure S3: Time dynamics (left) and phase-space portrait (right) of (B, S) solutions. Panels a,b: zero tree density. Panels c,d: Tree density $d = 0.3$, shading mechanism on. Panels e,f: Tree density $d = 0.3$, root mechanism on. Blue, red and black orbits denote precipitation levels of 150, 300 and 600 mm year^{-1} , respectively. The same eight initial conditions were used for all cases: $S = 0.2$ and B ranging from 0.1 to 0.8, with 0.1 increments. Hollow circles denote the value of the solution with initial condition ($B = 0.4, S = 0.2$) at time 500 days.

Crucially, the facilitation-to-competition switch persists when we examine transient dynamics, not only steady-state outcomes. In Fig. S4, we compare the steady-state pattern (panel a) with solutions obtained by integrating Eq. (1) for 180 days (panel b). The qualitative result is the same in both cases, with positive tree effects at low precipitation and negative effects at high precipitation. Temporal dynamics, however, alter the details: the magnitude of facilitation and competition, and the

⁷²⁸ precipitation at which the switch occurs, differ between transient and steady-state results.

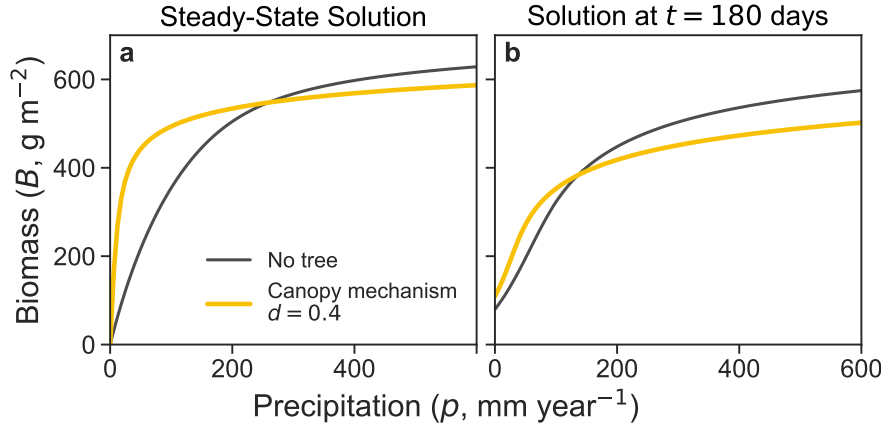


Figure S4: The transition from facilitation to competition, for steady-state solutions (panel a), and for transient solutions after 180 days (panel b). The initial conditions for the transient solutions are ($B = 200 \text{ g}$, $S = 0.2$). For both panels we considered only the canopy mechanism, for tree density levels 0.0 and 0.4. Other parameters as reported in Table 1.

⁷²⁹ S5 A gradient of evaporative demand

⁷³⁰ Here, we demonstrate that our model can produce a transition from facilitation to competition, not
⁷³¹ only along a precipitation gradient but also across an evaporative demand gradient (Figure S5)

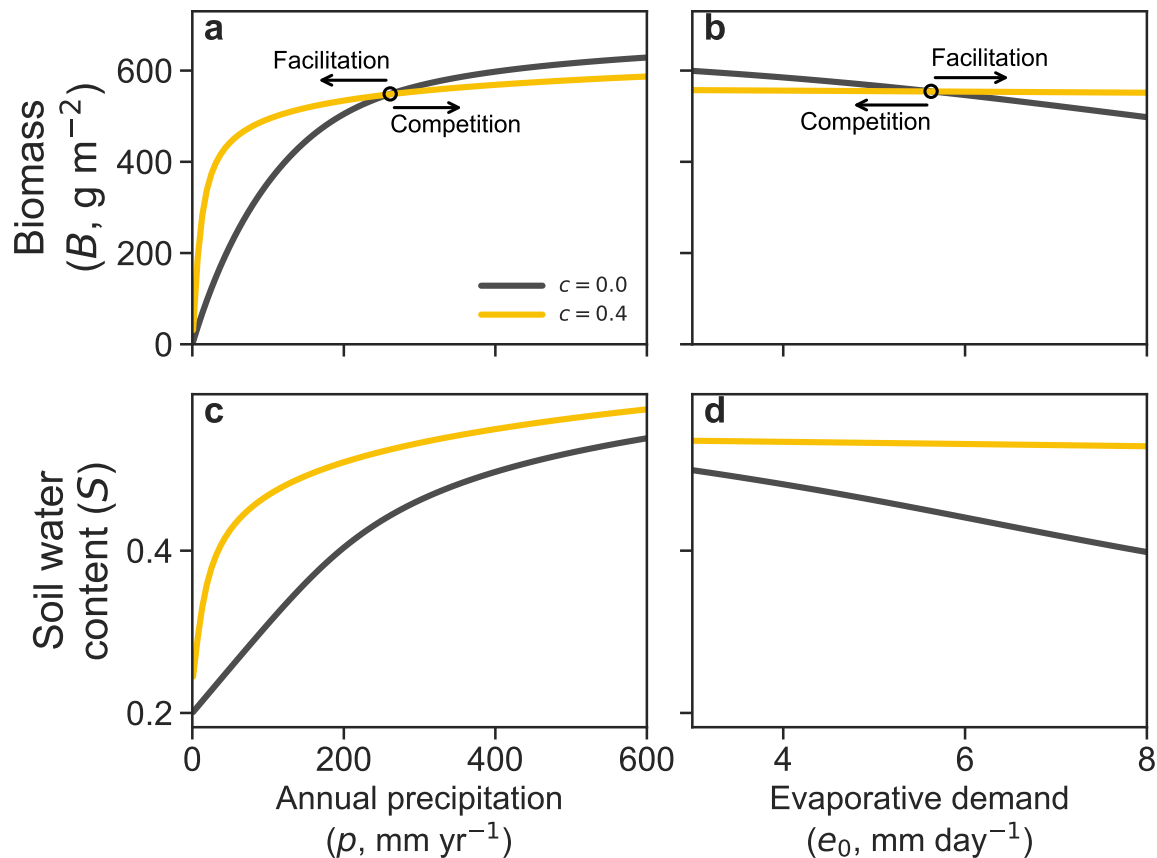


Figure S5: The facilitation–competition transition extends across different abiotic stress axes. Panels a,c: Precipitation as the stress axis reproduces the classic SGH prediction, with facilitation at low supply and competition at high supply. Panel b,d: Evaporative demand, representing atmospheric drivers of water loss, yields the same qualitative pattern but on a reversed axis (higher demand corresponds to stronger stress).

732 S6 Choosing the Right Resource Metric for the SGH

733 The Stress Gradient Hypothesis (SGH) predicts a shift from facilitation to competition as a resource
 734 increases. A critical question is which resource metric to use: resource supply rate (like precipitation)
 735 or resource abundance (like soil water content). We demonstrate here that the resource supply rate is
 736 the appropriate metric for assessing the SGH.

737 When we analyze our model using precipitation as the *control parameter* (x-axis in a B vs. p plot), the
 738 results clearly demonstrate the SGH pattern. For both the shading and root mechanisms, we observe
 739 a transition from positive to negative tree-herb interactions as precipitation increases, mirroring field
 740 observations.

741 In contrast, if we use soil water content as the resource metric, the SGH pattern vanishes. Figure S6
 742 shows the same herb biomass solutions as Figure 2, but plotted against soil water content.

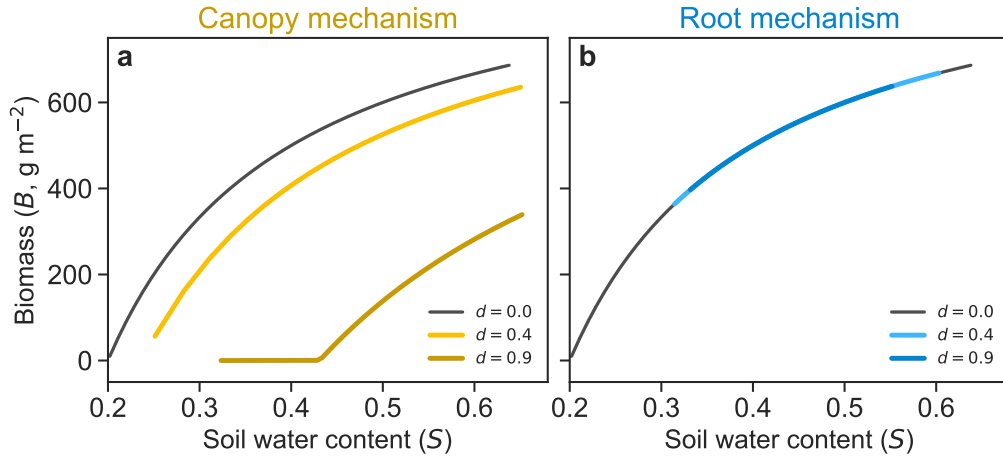


Figure S6: Using soil water content as the stress axis eliminates the facilitation–competition transition. Steady-state herb biomass solutions are shown as a function of soil water content for the canopy mechanism (panel a) and the root mechanism (panel b). In the canopy mechanism, biomass with trees ($d > 0$) is always lower than the no-tree baseline, because canopy directly reduces assimilation while water conservation effects are no longer represented. In the root mechanism, biomass becomes independent of tree density when soil water is fixed, since tree effects operate only by altering soil moisture levels. Accordingly, when stress is parameterized by soil water abundance rather than supply rate, the SGH pattern disappears.

743 The nontrivial ($B \neq 0$) solutions can be readily obtained by equating Eq. (1a) to zero and solving for
 744 B:

$$\text{Shading mechanism: } B^*(S) = k \left(1 - \frac{m}{aS f_a(d)} \right) \quad (\text{S7a})$$

$$\text{root mechanism: } B^*(S) = k \left(1 - \frac{m}{aS} \right) \quad (\text{S7b})$$

745 From these solutions we learn:

- 746 • **Shading mechanism:** Because $f_a(d > 0) < f_a(d = 0)$, the steady-state herb biomass
 747 with trees (B_T) is always lower than the biomass without trees (B_0). Trees always reduce light, which
 748 directly suppresses herb growth. Because the facilitative effect of water conservation is no longer
 749 a factor, the interaction intensity is always negative (competitive).
- 750 • **Root mechanism:** Herb biomass becomes completely independent of tree density (it lacks the
 751 variable d). Trees influence herbs solely by altering soil water levels, so if that level is fixed, the
 752 trees have no effect. The interaction intensity is always zero.

753 This result, that the SGH pattern disappears when using soil water content as the metric, occurs for a
 754 fundamental reason: soil water content, unlike precipitation, is an intrinsic property of the ecosystem,
 755 not an external force. It is the result of multiple processes such as rainfall, evapotranspiration,
 756 drainage, etc; all of which interact with the tree's presence to determine the final soil water content.
 757 By holding soil water constant, we are artificially decoupling the very mechanisms that create the
 758 SGH pattern. Therefore, using resource abundance (soil water content) as the metric of stress renders
 759 the SGH meaningless within this mechanistic framework, as it nullifies the resource component in our
 760 **consumer-resource model**.

761 The **resource supply rate** (precipitation) is the external driver of the system's state, making it the
 762 correct measure of abiotic stress for a resource-based SGH. It allows us to capture the full interplay of
 763 facilitative and competitive forces that are the core of the hypothesis.

764 S7 Logistic growth extension: nutrient-limited growth

765 To justify our choice of introducing a limiting factor to herb growth as a logistic term, we do the
 766 exercise of explicitly introducing a new essential resource, a nutrient N . Our model can be extended
 767 to include the nutrient dynamics as follows:

$$\frac{dB}{dt} = a f_a(d) B N S - m B \quad (\text{S8a})$$

$$n z_r \frac{dS}{dt} = p - e_0 f_e(d) B S - f_r(S, d) - q_s S^\gamma \quad (\text{S8b})$$

$$\frac{dN}{dt} = N_{\text{in}} - \mu N B - \nu N. \quad (\text{S8c})$$

768 The first equation, (S8a), describes the herb biomass dynamics, where we have replaced our original
 769 logistic term $f_k(B)$ with a nutrient term, N . Equation (S8c) describes the nutrient's dynamics, where
 770 it is introduced at a constant rate N_{in} , consumed by herbs (at a rate proportional to both herb biomass
 771 and nutrient availability, $\mu N B$), and lost from the system at a rate proportional to its own abundance,
 772 νN .

773 We now assume that the nutrient dynamics are much faster than those of the herb biomass (B) and
 774 soil water (S). We can therefore perform an adiabatic elimination by setting the rate of change of the
 775 nutrient to zero to find its quasi-steady-state:

$$0 = N_{\text{in}} - \mu N B - \nu N \quad (\text{S9a})$$

$$\Rightarrow N^* = \frac{N_{\text{in}}}{\nu} \frac{1}{\frac{\mu}{\nu} B + 1}, \quad (\text{S9b})$$

776 where N^* denotes the quasi-steady-state nutrient concentration. Substituting N^* into the herb biomass
 777 equation (S8a) gives:

$$\frac{dB}{dt} = a \frac{N_{\text{in}}}{\nu} f_a(d) B \left(\frac{1}{\frac{\mu}{\nu} B + 1} \right) S - m B. \quad (\text{S10})$$

778 The term in the parenthesis acts as a saturating function of B . When herb biomass is low, the term
 779 is close to one, and as biomass increases, the function decreases, effectively slowing the growth rate.
 780 This plays the same role as the logistic term we assumed in the main text.

781 To derive the exact logistic form, we can make an additional assumption. If we assume that the
 782 herbs are highly inefficient at consuming the nutrient relative to its decay rate ($\mu \ll \nu$), we can use a
 783 first-order Taylor series expansion:

$$\frac{1}{\frac{\mu}{\nu} B + 1} \approx 1 - \frac{\mu}{\nu} B. \quad (\text{S11})$$

784 Substituting this approximation into the herb biomass equation now reveals a classic logistic term:

$$\frac{dB}{dt} = a \frac{N_{\text{in}}}{\nu} f_a(d) B \left(1 - \frac{B}{k} \right) S - m B, \quad (\text{S12})$$

785 where the carrying capacity can be identified with $k = \nu/\mu$. If the factor N_{in}/ν is then incorporated
 786 into a , we get exactly Equation (1a) in the main text.

787 S8 Tree density dependent on precipitation

788 The arguments in Supplementary Section S1 stated that there can be no SGH transition in the absence
789 of a carrying capacity term for constant tree density. This picture changes if instead we allow for
790 precipitation-dependent tree density (as observed in many systems). Higher precipitation supports
791 greater tree density, which, in turn, exerts a stronger shading impact on herbaceous species. We
792 consider here two distinct functional forms of $d(p)$:

$$d(p) = \min\left(\frac{p}{1000}, 1\right) \quad (\text{S13a})$$

$$d(p) = \frac{p}{300 + p}. \quad (\text{S13b})$$

793 While the model internally uses p in mm d^{-1} , we present the equations $d(p)$ in mm y^{-1} for simplicity
794 and practical relevance.

795 Figure S7a illustrates the transition from facilitation to competition for these two functional forms.
796 Figure S7b shows the absolute interaction intensity in the (p, d) plane, and helps us interpret the
797 graph on the top. When a dark curve in the bottom panel crosses the border between facilitation
798 and competition, we see in the top panel that the dark curves cross the no-tree solution. For higher
799 values of d , when the dark curves in the bottom panel cross into the no-viable-biomass zone, we also
800 see a collapse of the vegetated solutions in the top panel. Finally, Fig. S7b helps us understand, from
801 another point of view, why there cannot be a transition from facilitation to competition in the case
802 of no carrying capacity and constant tree density, as previously discussed. Constant density solutions
803 (see for example the dotted line at $d = 0.2$) always cross from competition to facilitation as p increases,
804 never the other way around. By changing tree density from a constant value to increasing functions of
805 precipitation, as depicted by the solid dark lines, one can get the usual transition pattern of the SGH.

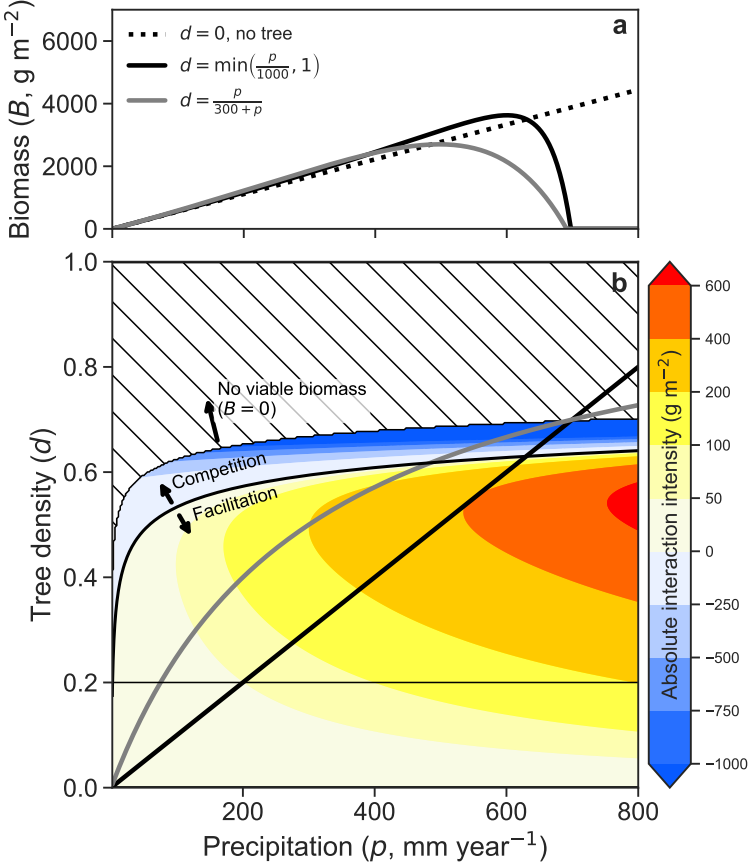


Figure S7: The Precipitation-Dependent Tree density Mechanism produces the SGH transition even without a carrying capacity term. Panel a: Steady-state herb biomass solutions (Eq. (S1b)) for a scenario without any tree density (dotted line) and for two possible instantiations of the tree-density dependence on precipitation (dark curves). Panel b: The absolute interaction intensity is shown in the (p, d) plane: warm colors denote positive interactions (facilitation), while cold colors denote negative interactions (competition). The hashed region in the top indicates no viable herb solutions ($B = 0$). The two functional forms for tree-density are plotted in solid dark curves. Parameters: $\beta_a = 0.9$ and $\beta_e = 1.1$, and other parameters as shown in Table 1.

806 S9 Infiltration

807 The infiltration mechanism is a variation of the canopy mechanism. In both, canopy shading
 808 reduces herb assimilation through $f_a(d)$; here, however, the facilitative pathway is not a reduction
 809 in evapotranspiration but an increase in effective infiltration as tree density rises. The model therefore
 810 keeps the growth-side shading term and replaces the rainfall input with an infiltrated input $p f_i(d)$:

$$\frac{dB}{dt} = a f_a(d) \left(1 - \frac{B}{k}\right) B S - m B, \quad (\text{S14a})$$

$$n z_r \frac{dS}{dt} = p f_i(d) - q_s S^\gamma - e_0 B S, \quad (\text{S14b})$$

811 The infiltration factor $f_i(d)$ follows ²:

$$f_i(d) = \frac{d + i_0 \delta}{d + \delta}, \quad (\text{S15})$$

812 so that $f_i(0) = i_0$ (minimum infiltration without trees) and $f_i(d) \rightarrow 1$ as d increases; see Fig. S8a.
 813 The parameter δ sets the density scale at which f_i is midway between i_0 and 1. Figure S8b shows the
 814 SGH transition for the infiltration mechanism.

815 This relationship captures the idea that canopy shading can suppress biological soil crusts (biocrusts),
 816 which often form a hardened surface layer that reduces infiltration. As tree density increases, shading
 817 limits biocrust activity and allows more water to infiltrate into the soil, thereby increasing the effective
 818 water supply to herbs.

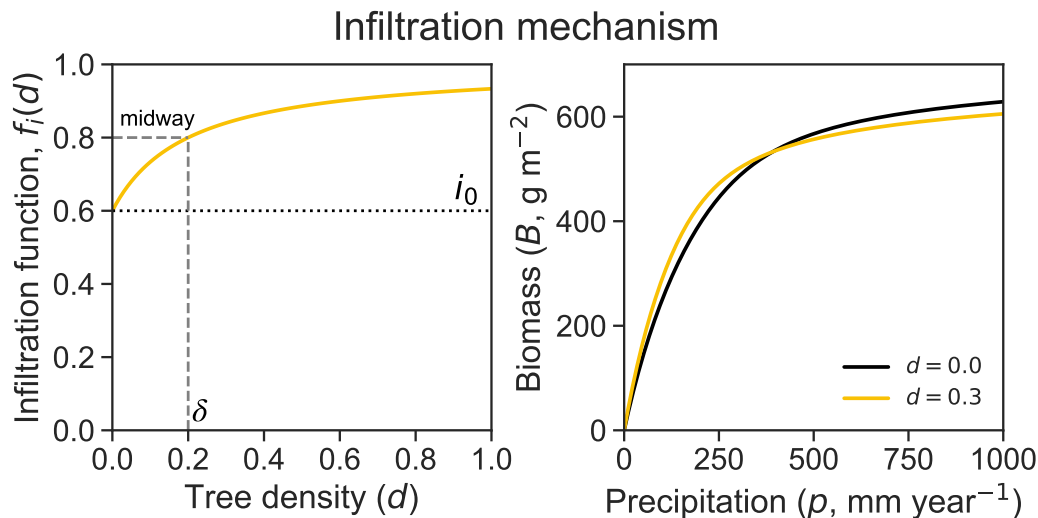


Figure S8: **Infiltration mechanism as a canopy variant.** (a) The infiltration factor $f_i(d)$ increases from i_0 at $d = 0$ toward 1 as tree density rises (δ controls the transition scale). (b) The transition from facilitation to competition can be obtained from the infiltration mechanism.

819 References

- 820 ¹ Tilman, D. (1982). *Resource Competition and Community Structure*. Princeton University Press,
 Princeton, NJ. <https://doi.org/10.2307/j.ctvx5wb72>
- 821 ² Gilad, E., von Hardenberg, J., Provenzale, A., Shachak, M., & Meron, E. (2004). Ecosystem
 engineers: from pattern formation to habitat creation. *Physical Review Letters*, 93(9), 098105.
<https://doi.org/10.1103/PhysRevLett.93.098105>